



**Controlling the velocity of air in the working section and in the body of a wind
tunnel**

التحكم في سرعة الهواء خلال منطقة الإختبار

وهيكل النفق الهوائي

By

Mohammed Saif Al Wahaibi

ID: 100130

A Dissertation submitted to the British University in Dubai in partial fulfilment of the requirements for the
Degree of MSc of the Systems Engineering

Faculty of Engineering & Information Technology

Dissertation Supervisor

Professor Robert Whalley

December 2015

Author Declaration

Candidate's SURNAME: Al Wahaibi.

Candidate's FORENAME: Mohammed Saif Salim.

Candidate's ID Number: 100130

DECLARATION

This work has not previously been accepted in substance for any degree and is not concurrently submitted in consideration for any other degree.

Signed..... Date.....

STATEMENT 1

This dissertation is being submitted in partial fulfillment of the requirements for the degree of MSc of the Systems Engineering.

Signed..... Date.....

STATEMENT 2

This dissertation is the result of my own independent work/investigation.

Signed..... Date.....

STATEMENT 3

I hereby give consent for my dissertation. If accepted, to be available for photocopying and for interlibrary loan, and for the title and a summary to be made available to outside organizations

Signed..... Date.....

© 2015

Mohammed Saif Salim Al Wahaibi ALL RIGHTS RESERVED

ABSTRACT

TITLE: Controlling the velocity of air in the working section and in the body of a wind tunnel

This dissertation deals with the multivariable control of an aircraft wind tunnel in order to find the simplest and most economical way of controlling the flow of air in the working section of a wind tunnel model. This model has two inputs, which are the fan motor and the ventilator vanes, and two outputs, which are the velocities in the form of multi input-output model. The comparison of the control methods used will be based on the assessment of the energy dissipated and the dynamic performance. The preferred control method of Least Effort Regulation will be assessed and related to the decoupling compensator method. Block diagrams of both methods and their plots will be included and step response transients and random noise assessment will be presented. The conclusion will state that the least effort control will be the best choice and a preferred method in terms of performance, economy, and energy dissipation from the results that are achieved.

تلخيص

العنوان: التحكم في سرعة الهواء في منطقة الاختبار وهيكل النفق الهوائي

يهدف هذا البحث الى إيجاد أفضل وأبسط وأقل طريقة تكلفة للتحكم في خروج الهواء عن طريقة قنوات الهواء, بحيث نضمن أداء أفضل وجهد أقل, مقدمة بحثي ستحدث عن النفق الهوائي وستتضمن المشاكل في متغيرات التحكم في سرعه الهواء في الجسم

هذا البحث يتحدث عن التعامل مع المتغيرات في طرق تصاميم التحكم للنفق الهوائي التي تكون بداخله المقصورات. يهدف البحث الى إيجاد ابسط و أسهل وأكثر الطرق إقتصادية للتحكم بمعنى أقل طاقة وأداء أفضل, طريقة التحكم تقارن بطرق أخرى سابقة في سياق الطاقه. سيتم ذكر مقدمة في النفق الهوائي في أول جزء من البحث , سيتضمن هذا البحث مشاكل في متغيرات التحكم في السرعه لجسم المروحة والجانب العملي فيها , هذا المتغير سيحتوي على قيمتين كمدخل ومخرج في النظام. سنقوم الدراسة بعرض مشروع الطاقة المتبدده واداء التحكم المقترح ومقارنته بطرق تحكم أخرى طبقا للقانون التقليدي والنظري. هذا البحث سيقوم بالمقارنة بين طريقتين وسيدعم بالرسم البياني وقيمهم. سوف يختم البحث بتوضيح أن التحكم في أقل جهد هي أفضل خيار لأفضل أداء وأقل تكلفة وأقل حاجة للطاقة من خلال النتائج التي توصلت لها التجارب من خلال البحث, هذه الطريقة مفيدة للتحكم في سرعة المروحة بدون الحاجة لإستهلاك طاقة كبيرة.

ACKNOWLEDGMENTS

I mostly thank my Uncle who has supported me through my university career.

I thank Prof. Whalley, who was my supervisor, and I am very proud to have applied his theory which served as the most practical method.

Dr. Alaa has guided me to presenting my dissertation and for that I am very grateful to have listened to his guidance.

Mrs. Mary Mayall was a great help in me writing better English and guiding me to know how the literature review should be done.

I would like to thank my wife who helped me organize my dissertation and providing me with everything I need that supports me with my work.

Mohammed Al Wahaibi

List of Notations and Abbreviations:

The definitions of all the variables that are used in this thesis are given below:

$a_{i,j}(s)$	Element of $A(s), 1 < i, j > m$
$a_{i,j}, b_{i,j}, \dots, Y_{i,j}$	Coefficients of $Q(s)$
$A(s)$	Numerator of $G(s)$
$b(s)$	Polynomial
b_0, b_1, \dots, b_{m-1}	Coefficients of $b(s)$
$d(s)$	Denominator of $G(s)$
f, f_1, f_2, \dots, f_m	Output loop feedback gains
F	Outer loop feedback array
$G(s)$	Transfer Function array (Input/Output)
H	Feedback path gain
$h(s)$	Feedback path Function
$H(s)$	Feedback path compensator model
I_m	Identify matrix
J	Performance index
K	Forward path gain
$k(s)$	Forward path function
$k > < h$	Outer product of k and h
$< k, h >$	Inner product of k and h
$K(s)$	Forward path pre-compensator model
L	Observer gain matrix

$L(s)$	Left(row) factors
n_1, n_2, \dots, n_m	Gain ratios
P	Pre-compensator array
Q	Coefficient array
S_s	Steady State input-output matrix
$y(s)$	Transformed output
ζ	Damping Ratio
T	Periodic Time
ω_d	Damped Natural Frequency
f	outer loop feedback gain
h_1	First Peak
h_2	Second Peak
ω_n	Natural Frequency
$K_p(s)$	Pre – Compensator
$K_d(s)$	Diagonal Matrix
K_c	Forward path compensator

LIST OF FIGURES

Figure 1.1: Process Variables

Figure 2.1: Benjamin Robins whirling arm assembly

Figure 2.2: The Wright Brother's Wind Tunnel

Figure 2.3: Gustave Eiffel's Wind Tunnel

Figure 2.4: Prandtl's Wind Tunnel

Figure 2.5: Elements of a Control System

Figure 2.6: Iron Heating Process

Figure 2.7: Step response example for the feed forward system

Figure 2.8: Proportional Control Energy cost for characteristic locus, Perron-Frobenius, INA and least effort controllers

Figure 2.9: Wind tunnel working section arrangement

Figure 2.10: Open loop response following a unit step change on reference input r_1

Figure 2.11: Open loop response following a unit step change on reference input r_2

Figure 3.1: root locus expression for equation 3.44

Figure 3.2: The Performance Index J against n

Figure 3.3: Block diagram representation of a Least Effort Controller for analysis purpose

Figure 3.4: The Conventional Structure of multivariable control system

Figure 4.1: Time domain of input 2 and output 2 for $f=0.5$ in least effort controller without reference input time delay

Figure 4.2: Decoupling control system

Figure 5.1: Close loop response following a unit step change on reference input r_1

Figure 5.2: Close loop response following a unit step change on reference input r_2

Figure 5.3: System response following a unit step change on ∂_1

Figure 5.4: System response following a unit step change on ∂_2

Figure 5.5: Close loop response following a unit step change on reference input r_1 for the decoupling compensator

Figure 5.6: Close loop response following a unit step change on reference input r_2 for the decoupling compensator

Figure 5.7: System response following a unit step change on ∂_1 for the decoupling compensator

Figure 5.8: System response following a unit step change on ∂_2 for the decoupling compensator

Figure 5.9: Proportional control energy costs following random distribution on disturbances 1 and 2 for the Least Effort Controller and the Decoupling Compensator.

TABLE OF CONTENT

Abstract.....	5
ملخص.....	6
Acknowledgments.....	7
List of Notations and Abbreviations.....	8
List of Figures.....	10
Table of content.....	12
Chapter 1: INTRODUCTION.....	14
1.1 Research Background.....	14
1.2 Research problem statement.....	15
1.3 Research Aims and Objective.....	16
1.4 Dissertation Organization.....	16
Chapter 2: LITERATURE REVIEW.....	17
2.1 Introduction to Wind Tunnel.....	17
2.1.1 Wind Tunnel Assembly.....	17
2.1.2 Wind Tunnel Types.....	18
2.1.2.1 Close Return Wind Tunnel.....	18
2.1.2.2 Open Return Wind Tunnel.....	19
2.2 Wind Tunnel Classification.....	19
2.3 Wind Tunnel Development History.....	19
2.4 Introduction to Control Systems.....	24
2.5 Control Systems Modeling.....	26
2.6 Time Domain Response.....	27
2.7 Control Theory.....	28
2.7.1 Optimal Control.....	29

2.8 Least Effort Control Method	30
2.9 Decoupling Compensator Control Method.....	31
2.10 The Design Model Chosen for Comparison.....	31
Chapter 3: Mathematical modelling using the least effort controller method.....	34
3.1 Least Effort Control Theoretical Equation.....	34
3.2 Least Effort Control Mathematical Modeling.....	39
Chapter 4: Mathematical modeling using the Decoupling compensator Control Method..	47
4.1 Graph Details.....	47
4.2 Forward Path Compensator Analysis.....	49
Chapter 5: Results Obtained.....	52
5.1 Results and Discussion.....	52
5.2 Summary.....	59
Chapter 6: Conclusion & Recommendation.....	60
6.1 Conclusion.....	60
6.2 Recommendation.....	60
REFERENCES.....	61

CHAPTER 1: Introduction

1.1 Research Background

Process engineers had a limited understanding of the devices that have feedback loops back in 1930. It was confusing to determine whether the feedback was positive or negative when applying control on certain systems. Additionally, theoretical knowledge was not available for the engineers, preventing them from designing such systems. Subsequently following World War 2, the interest in control systems grew dramatically (Bennet.S, 1993).

Albertos.P and Sala.A (2004) state that a control system is designed to manipulate the behavior of a system parameters. The behavior of the system can be determined by analyzing the stability of the outputs in the time domain. A system is said to be unstable if there is continuous oscillation in the time domain response. Disturbances occur during the control process and hence disturb its flow. Therefore the disturbance suppression is improved by minimizing the recovery time to quiescence. Energy dissipation analysis is a major concern in industrial plants. Less energy consumption leads to less maintenance time and a longer system life span. There are eight tasks that process engineers must accomplish to obtain a well behaved control system as will be outlined below:

1. Minimizing disturbance duration which indicates improved disturbance suppression.
2. Reference tracking to analyze the steady state error.
3. Detailing a sequential procedure for the system start-up and shutdown.
4. Tuning the multivariable parameters to obtain stability.
5. Changing operating conditions, structure or components to achieve performance improvement.
6. Avoiding any damage during the process by discovering any fault.
7. Providing the set-points
8. Obtaining information about the system performance.

The variables that accompany the system are used to study its behavior. As shown in figure 1.1 below, the variables include:

1. **External variables** including the manipulated inputs that are set by the engineer and the uncontrollable inputs which are the disturbances.
2. **Internal variables** including outputs, controlled variables and the state variables.

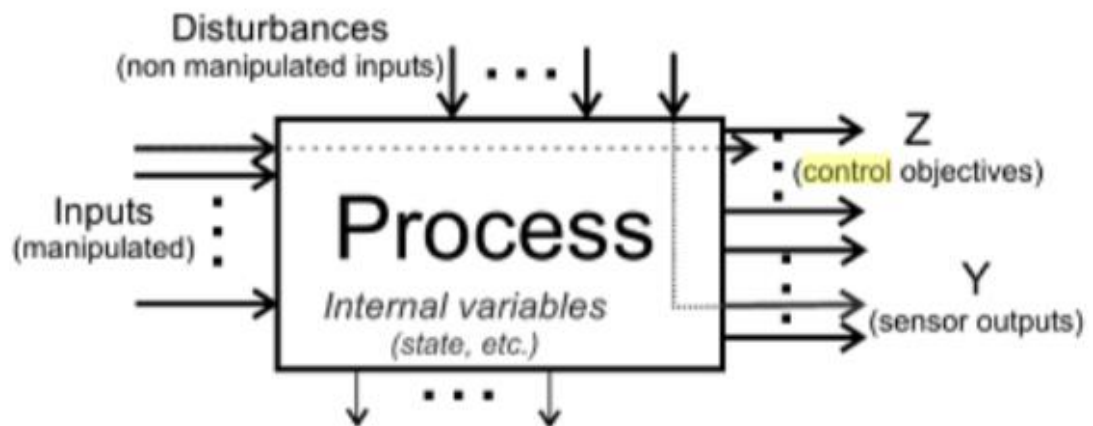


Figure 1.1: Process Variables

(Albertos.P and Sala.A, 2004)

1.2 Research problem statement

The main problem in this paper is the control of the air velocity in the working section and the body of the wind tunnel. A wind tunnel model which was derived by Whalley.R and Mitchel.D (1997) shall be presented in the research. The ventilator vane and the fan motor are the inputs and the pitot tubes measuring v_1 and v_2 are the outputs of the multivariable system.

Wind tunnel designers are concerned with the air speed generated from either the fan motor or angle change in ventilation vanes. Therefore, they need to be able to control the multivariable system to ensure the correct measurements on the test subject are accurately achieved. This will benefit the aircraft design procedure in order to restrict turbulence effects.

Additionally, the control energy dissipated is a very important issue in that the maintenance of the system is costly. That is why many methods of control are presented for the design of each system in order to find the least energy consumption for regulation purposes.

1.3 Research Aims and Objectives

The aim of the research is to apply the most efficient and cost effective method of control introduced by Whalley.R and Ebrahimi.M (2006) known as the least effort control, on the wind tunnel system model. This control theory attempts to have solution to achieve the transient and steady state responses, enhancing the disturbance suppression and limiting the response overshoot to 10 percent. The aim and objective of this research is to compare the least effort control method with decoupling control presented by Dutton.K, Thompson.S and Barraclough.W (1997) in the design of a controller in terms of energy dissipation efficiency, response and disturbance suppression.

1.4 Dissertation Organization

Chapter two will be concerned with the history of wind tunnel design and when and why wind tunnels were developed by engineers. It will be also shown how a model was derived from a current wind tunnel.

Chapter three will show the reader how least effort theory will be used for the controller design. The mathematical derivation will be included in this chapter. This chapter will also explain how the theory implemented to chapter four.

Chapter four explains the decoupling compensator method and will show how this method is impractical and consumes substantial energy.

Chapter five will show the implementation of two methods with results and comparisons. An explanation of how the results are implemented, will be included.

Chapter six will draw conclusions and give recommendations. It will give comparisons between the two methods with recommendations and reasons.

Chapter 2: Literature Review

2.1 Introduction to Wind Tunnels

Continuous airflow can cause vehicles such as aircrafts to become unstable. This instability occurs when vehicles are in motion. A lack of safety testing is the main reason for the widespread effects of airflow instability. In order to conduct a thorough structural safety inspection, Paraschivoiu.I (2003) states that a model must be tested in a controllable environment. These tests must be undertaken by engineers applying varying pressures, temperatures and dynamic forces at multiple speeds in order to observe changes in the fluid-body interactions. Engineers then use these findings to assess and predict the behavior and performance of models under various real-world conditions. These tests are mainly carried out in man-made structures called Wind Tunnels, which were created to simulate actual air flow conditions in a controlled environment.

2.1.1 Wind Tunnel Assembly

Every component in a wind tunnel assembly plays a role in the tunnel's overall ability to effectively examine structural integrity under varying airflow stresses.

Hussain.D and Hamid.A (2014) outlines the core components that make up the wind tunnel assembly as follows:

- a) ***Contraction Section and Testing Chamber:*** This chamber is designed to straighten the flow and make it laminar.
- b) ***Straightener:*** This part is used to convert turbulent airflow into a laminar flow before it enters the test section in order to avoid boundary layer growth, which affects test subject stability.
- c) ***Test Section:*** Also known as the "Working Section", this is where the test subject is mounted for performance testing.

- d) **Diffuser:** This part is used to change the laminar flow in the Test Section into a turbulent flow in order to match the shape of the mounted Motor Fan.
- e) **Motor Fan:** This fan is mounted at the end of the wind tunnel in order to counter the pressure loss that occurs while conducting performance testing on subjects.
- f) **Ventilating Vanes:** These vanes balance the pressure during testing in order to ensure optimal accuracy and minimize any distortion that may occur in the Test Section.
- g) **Pitot Tubes:** These are utilized to measure air velocity and the total pressure in the Working Section.
- h) **Static Tube:** This is used to analyze the static pressure in the Working Section and is "used with Pitot tube to measure the dynamic pressure at the boundary layer" (Hussain.D and Hamid.A 2014, p.108).
- i) **Pitot - static tube:** This combined transducer allows engineers to obtain various parameters such as speed, dynamic pressure and the static pressure of an air flow with zero viscosity at the core of the Working Section.
- j) **Micro Manometer:** An essential component for heating, ventilation and air conditioning systems (HVAC) monitoring, calibration or troubleshooting. It is also necessary for other pneumatic systems with the same purpose.
- k) **Traversing Mechanism:** This part is used to move the instruments mentioned earlier upwards and downwards according to the needs of the test.

2.1.2 Wind Tunnel Types

Two varieties of wind tunnels exist. These are Close Return Wind Tunnels and Open Return Wind Tunnels. The following sections will explain the characteristics of each type.

2.1.2.1 Close Return Wind Tunnel

Beyond its official name, the Close Return Wind Tunnel is often referred to as the Prandtl Tunnel after the German engineer – or the Gottingen Tunnel, referring to the German town in which it was first tested (Green.J and Quest.J 2011).

2.1.2.2 Open Return Wind Tunnel

The Open Return Wind Tunnel is also known as the Eiffel Tunnel, in honor of the French engineer, Gustav Eiffel (Green.J and Quest.J 2011).

2.2 Wind Tunnel Classification

Paraschivoiu.I (2003) classified wind tunnels in terms of speed, pressure and a parameter called the Mach number – a value that is proportional to the speed of air and inversely proportional to pressure. The Mach number increases if the speed of air is greater than the speed of sound. The following are explanations of the various wind tunnel classifications:

- a) Low Speed Wind Tunnel: Operating at a Mach number less than 0.3.
- b) Subsonic Wind Tunnel: Operating at a Mach number that is more than 0.3 and less than 0.9.
- c) Transonic Wind Tunnel: Operating at a Mach number between 0.8 and 1.2.
- d) Supersonic Wind Tunnel: Operating at a Mach number between 1.2 and 5.
- e) Hypersonic Wind Tunnel: Refers to any operation occurring at a Mach number that exceeds 5.

Miguel et al. (2013) state that wind tunnels were solely used in the past to test flying objects and vehicles until it was discovered that they have other applications on different test subjects. Nowadays, wind tunnels are also used to test various types of buildings and automobiles.

2.3 Wind Tunnel Development History

Wind Tunnels owe much of their developmental history to Benjamin Robins' experiments. The experiments involved musket balls – which are basic gun projectiles – being fired at different ranges with an adequate constant amount of powder prevalent. Different velocities of these musket balls were determined when these bullets became slow, the further they went. In 1746, Benjamin Robins developed the test subject experiment, which consisted of a whirling arm tightened to a drum at one side and a test subject on the other. A weight was also attached to the drum in order to move the whirling arm with the test subject, making it rotate

around the drum. The number of revolutions in a proposed time indicated the velocity of the test subject and the drag was denoted by the weight specified, that rotated the drum. As effective as the method was, it should be noted that high levels of accuracy were only achieved in slower test subjects. The figure below shows the assembly of the developed experiment (Green.J and Quest.J 2011).

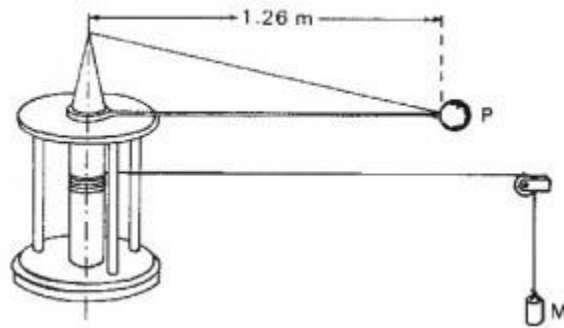


Figure 2.1: Benjamin Robins whirling arm assembly

(Green.J and Quest.J 2011)

In 1804, Sir George Cayley evolved Benjamin Robins' whirling arm device by replacing the ball with a square plate. The outcome of that study allowed him to build and fly a glider that was heavier than air. About a century later, between 1886 and 1889, another scientist, Otto Lilienthal used different whirling arm sizes in order to compare and determine how changing sizes affected the lift and drag specifications of airfoils.

Otto Lilienthal was skeptical about the accuracy of testing the airfoils using the whirling arm because it created a swirling wind effect. This effect recreated a very limited range of air conditions, which in Lilienthal's view, made the experiment inaccurate. Therefore, he opted for open ground experiments where natural wind conditions were uncontrolled and unpredictable, making the results more accurate for real world applications. Using the data from over 2500 glider flights, Lilienthal managed to create a table of calculations that went on to be of huge help to the Wright Brothers in their glider research in 1900 and 1901 (Green.J and Quest.J 2011). Sadly, Lilienthal died in 1896 after his glider took a nosedive during lift-off, leaving him with paralysis and breathing problems (Harsch.V, Bardrum.B and Illig.P 2008). The accident served

as a clear warning about the dangers of designers testing their own gliders in the field. The first wind tunnel was built by the Aeronautical Society (through British funding) in 1871 after Francis Wenham concluded that the whirling arm method was not accurate enough. The components of the first wind tunnel were very basic; according to the history, "It consisted of a duct 12 feet long with an 18 inch cross section and a fan upstream of the model, driven by a steam engine" (Green.J and Quest.J 2011). The first wind tunnel was an inferior design as it couldn't maintain a constant airflow – this meant that the results were not accurate during several airfoil experiments. Horatio Phillips designed a similar wind tunnel; his version featured a steam ejector, which made the airflow steadier – the steadier the airflow, the more accurate the measurements were. This development led to Phillips patenting the development of airfoils after creating a cambered airfoil (Green.J and Quest.J 2011). Cambered airfoils are superior to flat airfoils as they require 30% less energy dissipation to reach the lifting state of the airplane (Anderson.J 1997).

Realizing that Lilienthal's table of measurements was inaccurate, the Wright Brothers decided to build their own replica of Wenham's wind tunnel, as shown in the figure below. Using the repeatedly consistent data from their wind tunnel experiments, the Wright Brothers were able to improve their glider designs and even create a bigger, three-dimensional flight controller. It is my opinion (along with many experts in the field) that none of these achievements or the subsequent advancements in modern aircraft design would have been possible without the Wright Brothers' wind tunnel experiments and designs (Green.J and Quest.J 2011).



Figure 2.2: The Wright Brother's Wind Tunnel

(Green.J and Quest.J 2011)

The next notable wind tunnel development came in the 20th century when Gustave Eiffel built his first open return wind tunnel. This wind tunnel was instrumental in the construction of the world-renowned Eiffel Tower. The wind tunnel had the test section inside it as a vertical shaped area called "Salle D' Experiences" so he could test the behavior of his structure in it, as shown in the figure 2.3 next page. This advancement of the wind tunnel design enabled him to test a full sized aircraft indicating the success of the design especially on tall structures and large vehicles (Green.J and Quest.J 2011).

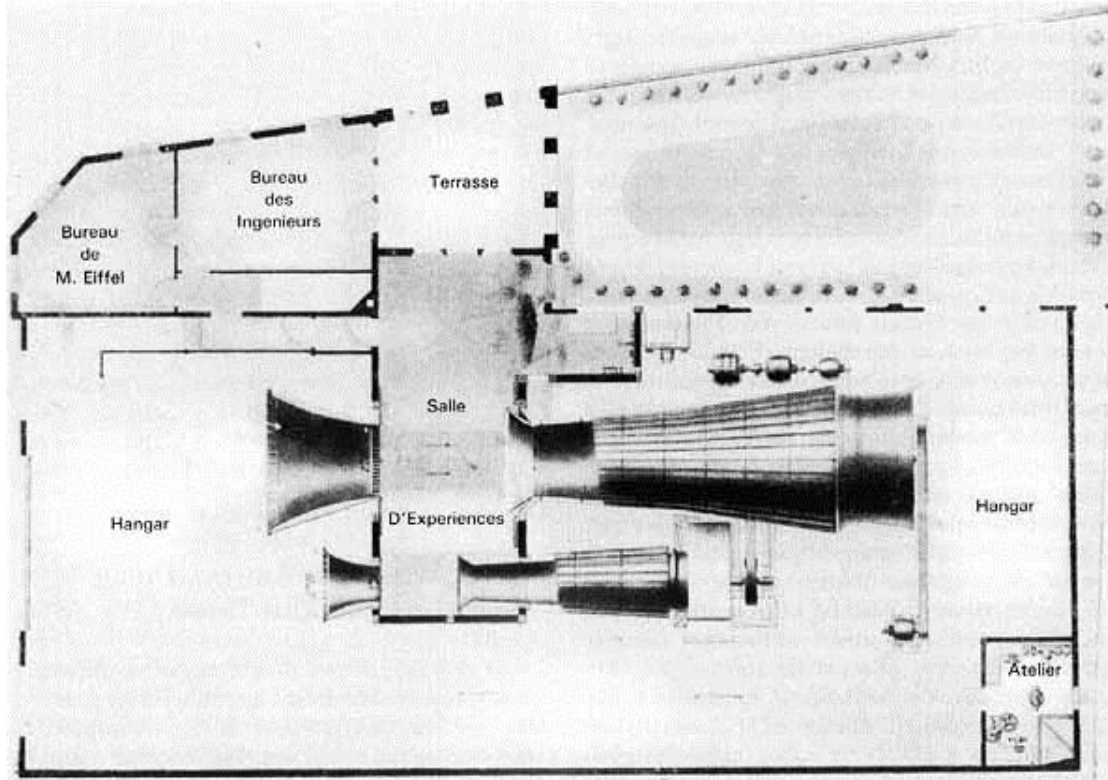


Figure 2.3: Gustave Eiffel's Wind Tunnel

(Green.J and Quest.J 2011)

As mentioned earlier, a scientist named Prandtl living in Gottingen, Germany, convinced the German Society for Airship Study to build another version of Eiffel's wind tunnel. This wind tunnel was to be a closed loop design, which was constructed from simple components. The basic components of Prandtl's wind tunnel were a fan, guide vanes in every corner to guide the wind inside it and a honeycomb shaped straightener. The straightener was used to reduce the turbulence of air created by the fan as it reaches the test subject. The problem with the first wind tunnel design was that the required air consistency could not be maintained when it reached the test subject. Prandtl suggested that a better designed wind tunnel be built. The War Administration approved his suggestion for construction after WWI (Green.J and Quest.J 2011).

The suggested wind tunnel had two more components with larger cross sectional areas. These two are the contraction and the diffuser. As explained above, the contraction compresses the air to making it laminar while facilitating more speed and a steadier flow. The diffuser is used to convert the laminar flow into the turbulent flow before the air goes into the fan.

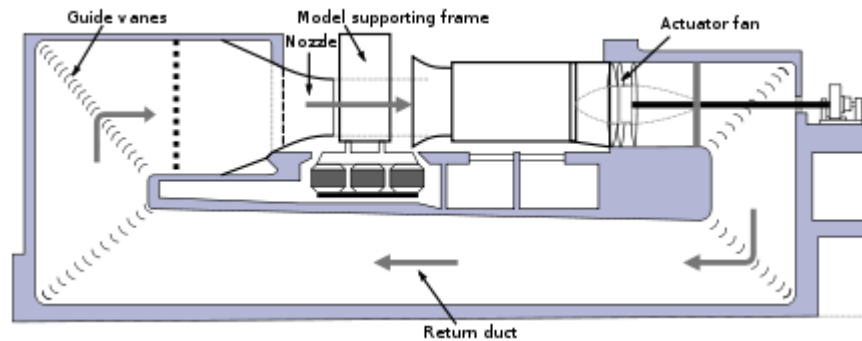


Figure 2.4: Prandtl's Wind Tunnel

(Green.J and Quest.J 2011)

These two components reduced the need for continuous fan power, which meant the dissipation of the energy is much lower than the first closed loop wind tunnel. This design is still in use today, and is very important in Formula 1 car design (Toet.W 2014).

A Ward-Leonard set is used for the fan system as "an AC motor driving a DC generator to supply the DC motor driving the fan. This gave accurate speed control over a range of 50 to 1100 rpm". (Green.J and Quest.J 2011).

2.4 Introduction to Control Systems

Dutton.K, Thompson.S and Barraclough.W (1997) describe a control system as an interface of the input and output regardless of the numbers of inputs and outputs. It consists of several elements that are typical in most of the designs for system modeling. These elements are as follows:

- a) Comparator: this component is used for point setting as a reference value to check the response behavior of a system in terms of stability, oscillations and steady state error.
- b) Compensator: A controller that is determined by the system model.
- c) Actuator: A component that is used to interface the compensator with the plant.
- d) Plant: Each plant has a model. This model determines the compensator design.
- e) Output Measurement: It is used as feedback enabling the comparison of the input and the formulation of the error

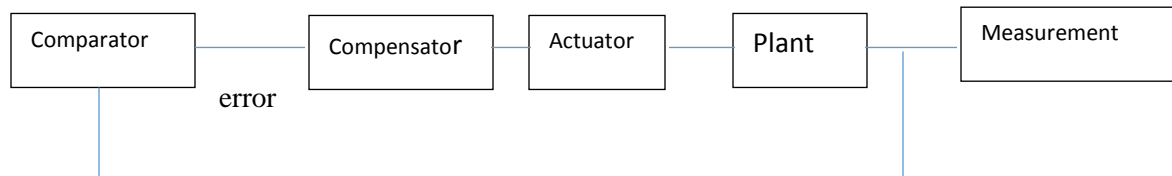


Figure 2.5: Elements in a Control System

There are two classifications of the control system – Open-Loop systems and Closed-Loop systems.

Dutton.K, Thompson.S and Barraclough.W (1997) define an Open-Loop system as a non-feedback system. This system has no automatic feedback wherein the system can correct any errors that might occur during the process. This means that the operator has to always check the process and manually correct for any errors or disturbances. It is also argued by Ghosh.S (2007) that there is no output measurement that can be identified from the system. A broom is given as an example when held vertically. The experiment controller cannot hold the broom vertically when blindfolded since the broom will fall if they are not able to see the broom location or status. Therefore, eye contact with the broom is very important, which will represent the feedback to the experiment controller who can see the status of the broom and act accordingly. When this is achieved, the system can be called a Closed-Loop system.

Ghosh.S (2007) states that the Closed-Loop system enables the designer to check the output status of the system and compare it to the desired input. This will enable the designer to correct any errors easily as explained in the previous example. A better example was given by Ghosh.S (2007) that more accurately relates to engineering wherein the comparator acts as a thermostat with the desired heat as the input. A controller in this system consists of a switch and

a heater and the plant acts as an iron that the system heats. The given iron temperature is the output of the system, where the experimenter can read and test it comparing the desired temperature with the actual temperature, using the thermostat, as shown in the figure below.

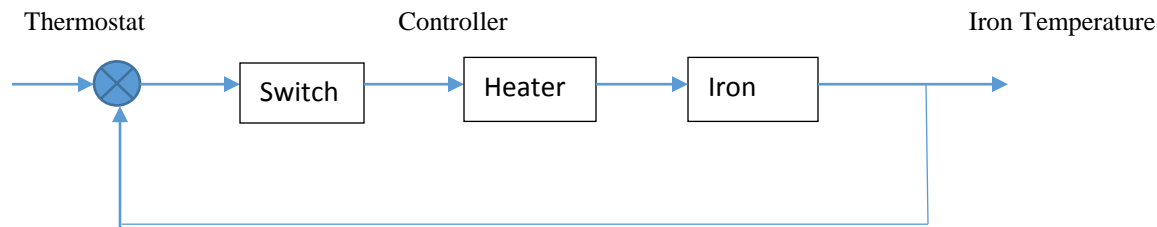


Figure 2.6: Iron Heating Process

This example explains how the lack of sensing devices limits the experimenter's ability to check for process errors, correct mistakes or reduce the risk of system instability since they won't be aware of any changes as they happen.

2.5 Control Systems Modeling

Given their vast experience on the subject of control system modeling, the work of Dutton.K, Thompson.S and Barraclough.W (1997) in the section will be cited. The main purpose of control systems modeling is to help design or define a particular system. Modeling systems can be categorized under two methodologies. The first methodology is focused on using system laws to identify the mathematical descriptions that define system behavior. This technique is called "Lumped Parameter Modeling" which means that the "control system can be represented by ordinary differential equations" (Ghosh.S 2007) that can then be derived into smaller orders for simplification. This method deals with the models that are yet to be designed and built. The second methodology involves describing system behavior through finding equations for models that are already in the field. Beyond finding parameter results that help describe mathematical models, this technique is useful when it comes to identifying areas of improvement in system accuracy, functionality and stability. This is an important function since all plants are prone to stability risks if operators do not monitor them properly. Therefore, control system modeling is essential because it enables the designer to understand the relationship between the systems' various inputs and outputs. The simple reality is that by changing the input parameters, the output results are also changed. Understanding this dynamic allows experimenters and designers

to improve system stability and accuracy depending on different needs. This relationship between inputs and outputs is crucial because it allows designers to identify the status of a system simply by comparing the output to the corresponding input. Therefore it is prudent to make the system as linear as possible or in other words to achieve "linearization" (Dutton, Thompson & Barraclough 1997).

2.6 Time Domain Response

It is essential to monitor how a system responds when applying a control so as to help the designer make any necessary corrections. This is why steady state error analysis is essential in this process as it determines the difference between the desired value and the actual value – also referred to as the input and output values, respectively (Dutton.K, Thompson.S and Barraclough.W 1997). Delving deeper into this subject, the steady state error shows the accuracy of the performance depending on the difference between the input and the output. This means the smaller the input-output gap the more accurate the system. Another parameter is the transient response. The transient response reaches zero state when time tends to the infinity ($t \rightarrow \infty$) depending on the oscillation state of the system. The example in the next page illustrates this occurrence enabling and understanding of the results as shown by the mathematical calculations in the forthcoming chapter.

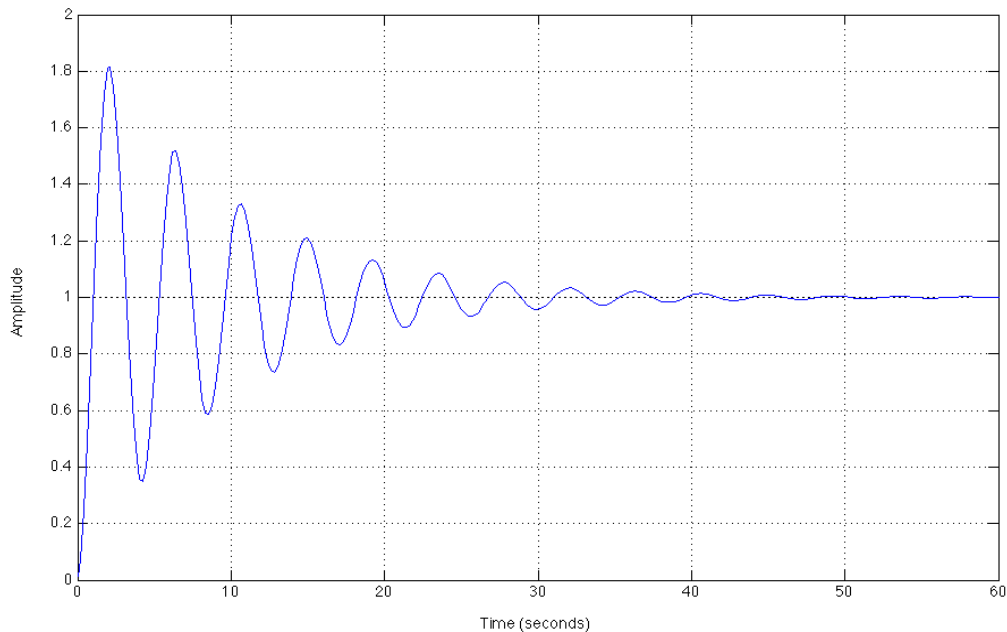


Figure 2.7: Step response example for the feed forward system

The figure above illustrates the process of a certain system with a stable, transient response. As can be observed, the system has many oscillations. The steady state error of the system is at zero after 60 seconds, indicating that the system reaches quiescence after 60 seconds. The time taken to reach the steady state is called the settling time. The lesser the oscillations, the better the system is in practice. The percentage overshoot is the first amplitude and is considered as high as 80%. This result is achieved by calculating each 0.1 as 10%. The rise time is indicated by the time the system reaches its peak from the start, and it is shown here that it is approximately 2 seconds. The rise time indicates how responsive the system is during the control process (Dutton.K, Thompson.S and Barraclough.W 1997).

2.7 Control Theory

There are two control theories that are applied on plants. Choosing each theory depends on the nature of the plant itself. Classical Control Theory can be applied to Single Input Single Output (SISO) linear and time-invariant systems, which are based on the Laplace Transform. The inputs and outputs of the system are related through a transfer function, which is defined by control needs of a particular plant model. Unlike Classical Control Theory, Modern Control

Theory uses a state variable approach. State variables can be obtained depending on the characteristic parameters of the system in order to form a transfer function matrix that includes several inputs and outputs (Burghes.D and Graham.A 1980) .

Gopal.M (1993) explained the history of Control Systems Theory development in the 1940s. Servomechanism was a newly developed technology wherein transient performance was very important because it involved tracking systems. For example, a gun uses the radar to follow the target in order to take an accurate shot. The advent of this technology along with the establishment of time domain theories in the field of Communication Engineering has helped control engineers obtain Nyquist's results, which were instrumental in designing highly accurate military devices and weapons with high quality transient response rates. W.R Evens is credited with adding the "Root Locus" technique to the time domain theory in system design, which helped complete the first developmental phase of control systems. The combination of the two techniques formed the basis of Classical Control Theory. However, this theory could not be used for complex systems (known as multivariable systems), which aerospace engineers began using in the 1950's.

2.7.1 Optimal Control

Many systems are costly to operate due to their dependence on electrical power. Therefore, it is essential to find an economical solution for operation in order to ensure low maintenance costs and longevity. The Optimal Control Theory has helped achieve a lot of developmental progress in terms of system design because of its ability to identify the signal process, overcome the constraints of system model equations and minimize the performance costs whilst maximizing performance accuracy. The Optimal Control minimizes the quadratic performance index and always gives a conservative response. The major problem in a system is lowering the rise time and settling time, which means increasing the response speed. This not only dissipates a high amount of energy, but it also requires extensive and frequent maintenance which is costly. This is the chief constraint that the system is facing during the process. Optimal controller designs are dictated by the state variables, which are derived from the parameters of the system (Dutton.K, Thompson.S and Barraclough.W 1997).

2.8 Least Effort Control Method

Whalley.R and Ebrahimi.M (2006) introduced the least effort controller as a design method that is concerned with creating a controller that requires the least amount of energy whilst still remaining accurate and stable. The design would show the required disturbance suppression and how to minimize the output interaction when applying the disturbance on the system, which is an important function as the system, needs to have a quick disturbance recovery when it occurs. The method will require minimal energy consumption, which means minimal maintenance costs, heating, noise pollution and vibration, meaning that the overall operational expenditure is extremely efficient. The method was applied on various systems to prove its validity and effectiveness. The figure below shows a different system as an example for energy efficiency. This experiment was conducted by Whalley.R and Ebrahimi.M (2006).

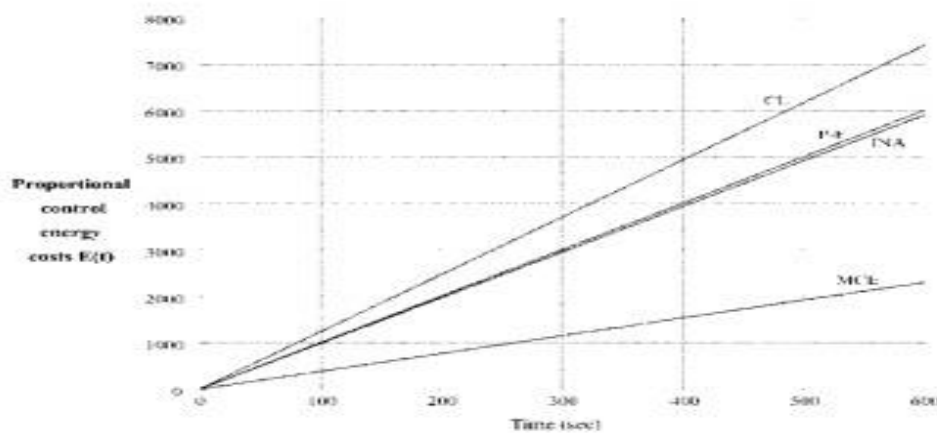


Figure 2.8: Proportional Control Energy cost for Characteristic Locus (CL), Perron-Frobenius (PF), Inverse Nyquist Array (INA) and Minimum Control Effort (MCE)

(Whalley.R and Ebrahimi.M 2006)

Figure 2.8 shows that the Characteristic Locus Method consumes more energy than other methods while the Least Effort Control Method has the least energy consumption.

2.9 Decoupling Compensator Control Method

The Decoupling Compensator method was illustrated by Dutton.K, Thompson.S and Barraclough.W (1997) as mentioned in chapter one. This is chosen for comparison purposes with the Least Effort Controller. This method uses the pre-compensator along with the diagonal matrix to form the overall plant decoupling compensator for the system design. The pre-compensator is formed by finding the inverse matrix of the given transfer function matrix as will be shown in the mathematical model of the system. In order for the overall compensator to be formed for the design, the required parameters need to be computed from the system as will be illustrated in the next chapter – these parameters are the natural frequency and the damping ratio of the system. However, the problem in this method will be shown in the modeling and in the results wherein the system uses high order polynomial functions for controlling the two wind tunnel velocities. The use of this method demonstrates to the reader the impracticality of this method as opposed to the Least Effort Controller.

2.10 The Design Model Chosen for Comparison

In this chapter, the Least Effort Control Method (the proposed method) and the Decoupling Compensator Method will be compared in terms of transient response, disturbance suppression and energy cost. The two methods have different calculations and different transient responses to be compared as well.

In this paper, both methods will be applied to the wind tunnel's body and the working section, and specifically on the fan motor and the ventilating vanes to control the speed of the air flow created by the fan. Figure 2.11 shows the assembly of the wind tunnel's working section design, which will be used in this paper for the two methods mentioned earlier.

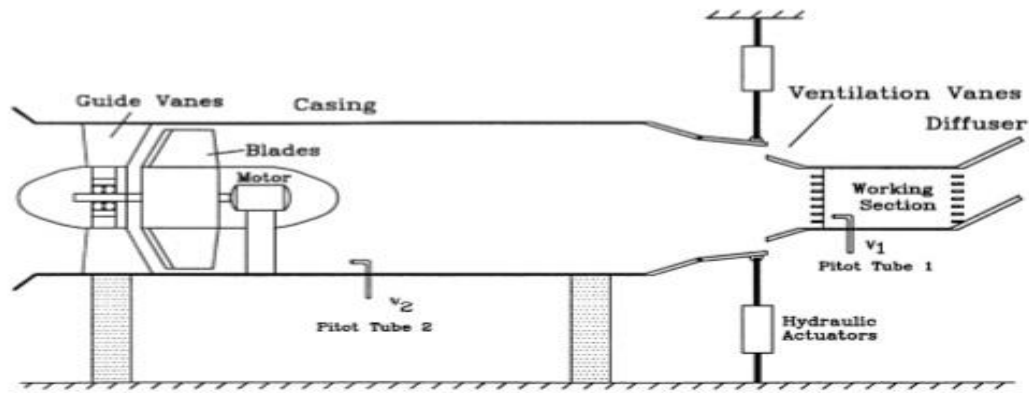


Figure 2.9: Wind tunnel working section arrangement

(Whalley.R and Mitchell.D, 1997)

The velocities v_1 and v_2 are measured by using the pitot tubes mounted at the locations shown in the figure. Whalley.R and Mitchell.D (1997) have given the model for this wind tunnel according to their analysis and the transfer function matrix was:

$$G(s) = \begin{bmatrix} \frac{1}{s^2+4s+8} & \frac{0.5(s-4)}{(s+4)(s^2+4s+8)} \\ \frac{2}{(s+8)(s^2+4s+8)} & \frac{s+1}{(s+8)(s^2+4s+8)} \end{bmatrix}$$

This model transfer function matrix of the wind tunnel will be used in the design of the two control methods mentioned earlier.

Whalley.R and Mitchell.D (1997) argue that the sudden drop in the pressure will occur when changing the ventilator vane angle. This will affect the velocity in v_1 for a short period of time before returning to the steady state. This will be shown in the results of the open-loop system and also when applying the least effort control theory.

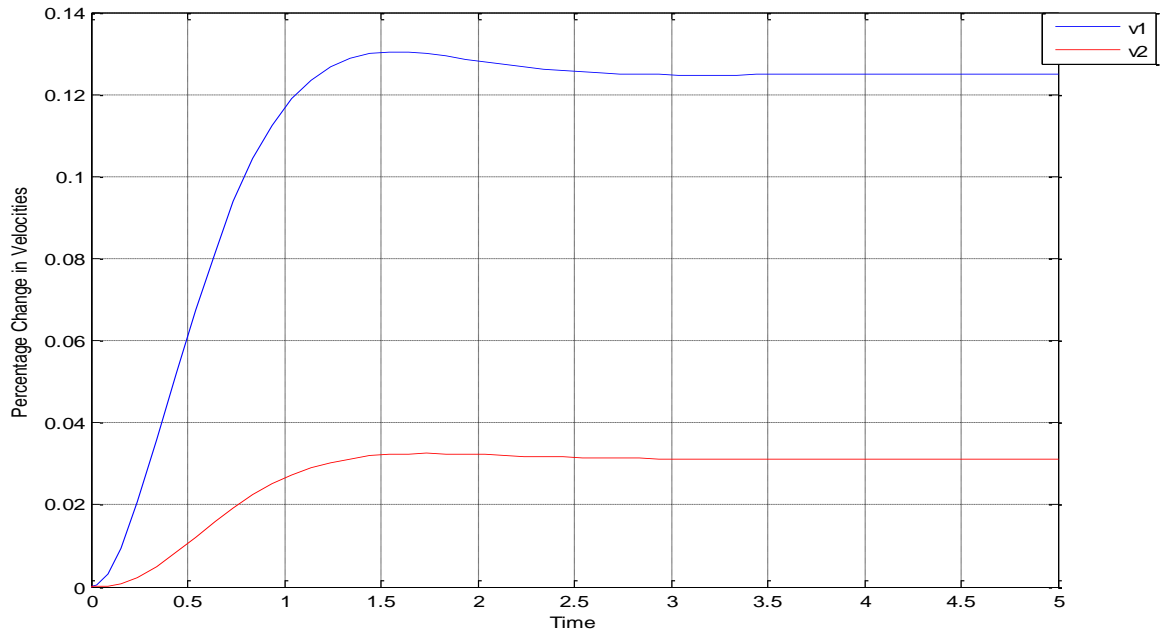


Figure 2.10: Open loop response following a unit step change on reference input r_1

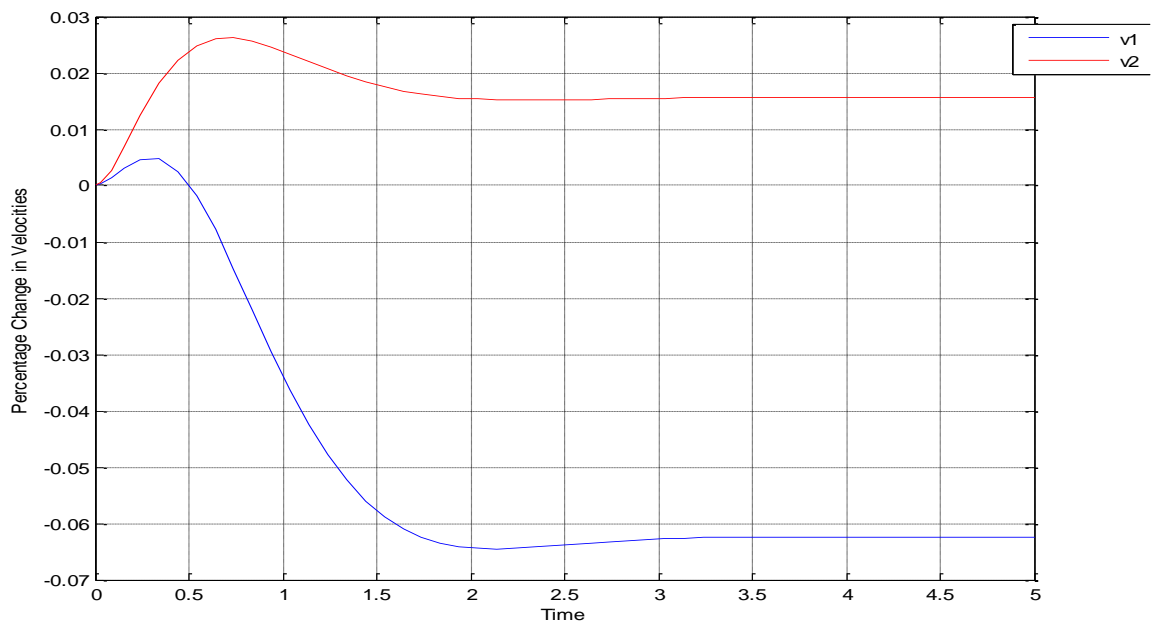


Figure 2.11: Open loop response following a unit step change on reference input r_2

Chapter 3: Mathematical modelling using the least effort controller method

3.1 Least Effort Control Theory

In this section, the equations for the least effort control method will be outlined. These equations will ensure that there are few oscillations before steady state conditions and also secure low frequency disturbance output conditions.

The open loop equation is:

$$y(s) = G(s)u(s) + \delta(s) \quad 3.1$$

and the control law is:

$$u(s) = k(s)[\bar{r}(s) - h(s)y(s)] + P(r(s) - Fy(s)) \quad 3.2$$

Hence the closed loop equation is:

$$y(s) = (I_m + G(s)(k(s) >< h(s) + PF))^{-1} \times (G(s) Pr(s) + \delta(s)) \quad 3.3$$

In Equation 3.3, $\|G(s)(k(s) > h(s) + PF)\|_\infty$ if finite for all s on the D contour, so if steady state matrix S_s is selected such that

$$y(0) = S_s r(0)$$

Then from equation 3.3 with $\delta(s)$ zero

$$P = (G(0)^{-1} + k(0) >< h(0))S_s(I - FS_s)^{-1} \quad 3.4$$

If the diagonal elements of S_s are unity and the off diagonal elements are less than 1, then for closed loop non-interaction with $S_s=I$ and substituting for \mathbf{P} from equation 3.4 results in equation 3.3 becoming.

$$y(s) = \{I_m + G(s)[k(s) >< h(s) + (G(0)^{-1} + k(s) >< h(s))(I_m - F)^{-1}F]\}^{-1} \times \{G(s) Pr(s) + \delta(s)\} \quad 3.5$$

At low frequencies:

$$G(s)P \cong \frac{1}{1-f} (I_m + G(s)k(0) \succ \prec h(0))$$

and after achieving the steady state, equation 3.5 becomes

$$y(s) = I_m r(s) + S(s)\delta(s) \tag{3.6}$$

where at low frequency sensitivity matrix

$$S(s) = (1-f)(I_m + G(s)k(s) \succ \prec h(s))^{-1}, 0 < f < 1$$

It can be seen from equation 3.6 that steady state non-interaction to input references changes will be achieved and if f is increased, the steady state disturbance rejection will be increased as well.

From equation 3.3 and since forward path $\mathbf{K}(s)$ and feedback path compensator $\mathbf{H}(s)$ are needed for the implementation purpose, then the following equation can be used.

$$y(s) = (I_m + G(s)K(s)H(s))^{-1} [GK(s)r(s) + \delta(s)] \tag{3.7}$$

and by comparing equations 3.3 and 3.7 it is found that

$$K(s) = P \tag{3.8}$$

$$K(s)H(s) = k(s) \succ \prec h(s) + PF$$

So that

$$H(s) = P^{-1}k(s) \succ \prec h(s) + F \tag{3.9}$$

In the Inner loop analysis, the following equation is the Laplace transformed open-loop system which is given by equation 3.1

$$\mathbf{G}(s) = \mathbf{L}(s) \frac{\mathbf{A}(s)}{d(s)} \mathbf{R}(s) \mathbf{\Gamma}(s) \quad 3.10$$

where

$$\mathbf{L}(s) = \mathbf{Diag} \left(\frac{\lambda_j(s)}{p_j(s)} \right)$$

And

$$\mathbf{R}(s) = \mathbf{Diag} \left(\frac{\rho_j(s)}{q_j(s)} \right)$$

$$\mathbf{\Gamma}(s) = \mathbf{Diag}(e^{-sT_j}), 1 \leq i, j \leq m$$

$\mathbf{A}(s)$ is a non-singular matrix rational functions and the determinant can't be equal to zero with elements

$$a_{ij}(s) = a_{ij}s^{m-1} + b_{ij}s^{m-2} + \dots + \gamma_{ij} \quad 1 \leq i, j \leq m \quad 3.11$$

As the transformed input-output relationship is

$$y(s) = G(s)u(s) + \delta(s) \quad 3.12$$

The inner-loop control law is

$$u(s) = k(s)[\bar{r}(s) - h(s)y(s)] \quad 3.13$$

Combining the two previous equations will give

$$y(s) = (I_m + G(s)k(s) >< h(s))^{-1}(G(s)k(s)\bar{r}(s) + \delta(s)) \quad 3.14$$

The order of the finite time delays in $\mathbf{\Gamma}(s)$ may be organized as $T_i \geq T_j, 1 \leq j \leq m, i \neq j$ and for that, the gain vector can be arranged with

$$k(s) = [k_1(s)e^{-s(T_i-T_j)}, k_2(s)e^{-s(T_i-T_j)} \dots, k_1(s), \dots, k_m(s)e^{-s(T_i-T_j)}]^T \quad 3.15$$

because

$$h(s) = (h_1(s), h_2(s), \dots, h_m(s)) \quad 3.16$$

If $k_j(s) = k_j \phi_j(s)$ and $h_j(s) = h_j \mathcal{X}_j(s)$ $1 \leq j \leq m$

where $\phi_j(s)$ and $\mathcal{X}_j(s)$ are proper or strictly proper stable phase functions and when selected, equation 3.14 will become

$$y(s) = \left(I_m + e^{-sT_i} n(s) L(s) \frac{A(s)}{d(s)} k(s) \right)^{-1} \times \left(n(s) L(s) \frac{A(s)}{d(s)} k e^{sT_i} r(s) + \delta(s) \right) \quad 3.17$$

where

$$k = (k_1, k_2, \dots, k_m)^T \quad 3.18$$

$$h = (h_1, h_2, \dots, h_m) \quad 3.19$$

and

$$d(s) = s^k + a_1 s^{k-1} + \dots + a_0$$

Also

$$\deg \left(n(s) a_{i,j}(s) \right) < k \quad 1 \leq i, j \leq m$$

The determinant of equation 3.17 is

$$\det \left[I_m + e^{-sT_i} n(s) L(s) \frac{A(s)}{d(s)} k(s) \right] = 1 + e^{-sT_i} n(s) \left\langle h \frac{A(s)}{d(s)} k \right\rangle \quad 3.20$$

The inner product of this equation is

$$\left\langle h A(s) k \right\rangle [1, s, \dots, s^{m-1}] \begin{bmatrix} \gamma_{11} & \gamma_{12} & \dots & \gamma_{mm} \\ \vdots & \vdots & \ddots & \vdots \\ b_{11} & b_{12} & \dots & b_{mm} \\ a_{11} & a_{12} & \dots & a_{mm} \end{bmatrix} \begin{bmatrix} k_1 h_1 \\ k_2 h_2 \\ \vdots \\ k_m h_m \end{bmatrix} \quad 3.21$$

Obtaining the gain ratios in equation 3.21 results the following equation

$$k_2=n_1k_1, k_3=n_2k_1\dots\dots\dots, k_m=n_{m-1}k_1 \quad 3.22$$

$$\langle \mathbf{hA}(s)\mathbf{k} \rangle = b(s) \quad 3.23$$

The equation implies that

$$\mathbf{k}_1[\mathbf{Q}]\mathbf{h} = (b_{m-1}, b_{m-2}, \dots, b_0)^T \quad 3.24$$

where

$$Q = \begin{bmatrix} \gamma_{11} + \gamma_{12}n_1 + \dots + \gamma_{1m}n_{m-1} \dots & b_{21} + b_{22}n_1 + \dots + b_{2m}n_{m-1} \dots \\ \vdots & a_{21} + a_{22}n_1 + \dots + a_{2m}n_{m-1} \dots \\ b_{11} + b_{12}n_1 + \dots + b_{1m}n_{m-1} \dots & \gamma_{m1} + \gamma_{m2}n_1 + \dots + \gamma_{mm}n_{m-1} \\ a_{11} + a_{12}n_1 + \dots + a_{1m}n_{m-1} \dots & b_{m1} + b_{m2}n_1 + \dots + b_{mm}n_{m-1} \\ \gamma_{21} + \gamma_{22}n_1 + \dots + \gamma_{2m}n_{m-1} \dots & a_{m1} + a_{m2}n_1 + \dots + a_{mm}n_{m-1} \end{bmatrix}$$

The control effort at time t is proportional to

$$(|k_1h_1| + |k_2h_1| \dots |k_mh_1|)|y_1(t)| + (|k_1h_2| + \dots + |k_mh_2|)|y_2(t)| + \dots + (|k_1h_m| + |k_2h_m| + \dots + |k_mh_m|)|y_m(t)|$$

Then the energy cost are proportional to

$$E(t) = \int_{t=0}^{t=T_f} (\sum_{i=1}^m k_i^2 \sum_{j=1}^m h_j^2 y_j^2(t)) dt \quad 3.25$$

Minimum $E(t)$ for arbitrary $y_1(t)$ requires that J should be minimizes where:

$$J = \sum_{i=1}^m k_i^2 \sum_{j=1}^m h_j^2 \quad 3.26$$

Hence

$$J = (k_1)^2(1 + n_1^2 + n_2^2 + \dots + n_{m-1}^2)(h_1^2 + h_2^2 + \dots + h_m^2) \quad 3.27$$

and from equation 3.24:

$$\mathbf{h} = \mathbf{k}_1^{-1}\mathbf{Q}^{-1}\mathbf{b}$$

So that: 3.28

$$J = (1 + n_1^2 + n_2^2 + \dots + n_{m-1}^2)b^T(Q^{-1})^T Q^{-1}b \quad 3.29$$

The disturbance the response is given by

$$y(s) = S(s)\delta(s) \quad 3.30$$

where

$$S(s) = (I_m + G(s)k(s) >< h(s) + PF)^{-1} \quad 3.31$$

3.2 Least Effort Control

In this section the application of the theoretical equations for the proposed control method will be shown as follows:

$$G(s) = \begin{bmatrix} \frac{1}{s^2 + 4s + 8} & \frac{0.5(s - 4)}{(s + 4)(s^2 + 4s + 8)} \\ \frac{2}{(s + 8)(s^2 + 4s + 8)} & \frac{s + 1}{(s + 8)(s^2 + 4s + 8)} \end{bmatrix} \quad 3.32$$

$$G(s) = L(s) \cdot A(s) \quad 3.33$$

Where

$$L(s) = \begin{bmatrix} \frac{1}{(s + 4)} & 0 \\ 0 & \frac{1}{(s + 8)} \end{bmatrix} \quad 3.34$$

$$A(s) = \begin{bmatrix} \frac{s + 4}{s^2 + 4s + 8} & \frac{0.5(s - 4)}{s^2 + 4s + 8} \\ \frac{2}{s^2 + 4s + 8} & \frac{s + 1}{s^2 + 4s + 8} \end{bmatrix} \quad 3.35$$

$$A_{(s)} = \frac{\begin{bmatrix} s+4 & 0.5(s-4) \\ 2 & s+1 \end{bmatrix}}{(s^2 + 4s + 8)} \quad 3.36$$

$$I + GK \gg h = 1 + hGK$$

$$\left[\left(\frac{s+4}{s+8} \right) h_1, h_2 \right] \begin{bmatrix} \frac{1}{s+4} & 0 \\ 0 & \frac{1}{s+8} \end{bmatrix} \frac{\begin{bmatrix} s+4 & 0.5(s-4) \\ 2 & s+1 \end{bmatrix}}{s^2 + 4s + 8}$$

Hence:

$$= \left([h_1, h_2] \frac{\begin{bmatrix} s+4 & 0.5(s-4) \\ 2 & s+1 \end{bmatrix}}{(s+8)(s^2 + 4s + 8)} \begin{bmatrix} k_1 \\ k_2 \end{bmatrix} \right) \quad 3.37$$

The denominator of equation 3.37 is:

$$d_{(s)} = s^3 + 12s^2 + 40s + 64 \quad 3.38$$

and

$$J = \frac{\begin{bmatrix} 1 & s \end{bmatrix}}{d_{(s)}} \begin{bmatrix} 4 & -2 & 2 & 1 \\ 1 & 0.5 & 0 & 1 \end{bmatrix} \begin{bmatrix} k_1 h_1 \\ k_2 h_1 \\ k_1 h_2 \\ k_2 h_2 \end{bmatrix} \quad 3.39$$

$$k_1 = 1, \quad k_2 = nk_1 = n$$

$$J = \frac{\begin{bmatrix} 1 & s \end{bmatrix}}{d_{(s)}} \begin{bmatrix} 4 & -2 & 2 & 1 \\ 1 & 0.5 & 0 & 1 \end{bmatrix} \begin{bmatrix} h_1 \\ nh_1 \\ h_2 \\ nh_2 \end{bmatrix} \quad 3.40$$

$$\left(\frac{h_{(s)} A_{(s)} K}{d_{(s)}} \right) = \frac{\begin{bmatrix} 1, s \end{bmatrix}}{d_{(s)}} \begin{bmatrix} 4 - 2n & : & 2 + n \\ 1 + 0.5n & : & n \end{bmatrix} \begin{bmatrix} h_1 \\ h_2 \end{bmatrix} \quad 3.41$$

For determining the gain b_0

$$J = k_1^2 (1 + n^2)(h_1, h_2) \begin{pmatrix} h_1 \\ h_2 \end{pmatrix} \quad 3.42$$

and

$$J = k_1^2 (1 + n^2)b_0(x - 1) (Q^{-1})^T Q^{-1} \begin{pmatrix} x \\ 1 \end{pmatrix} b_0 \quad 3.43$$

so that

$$\frac{b_0(s + x)}{s^3 + 12s^2 + 40s + 64} = -1 \quad 3.44$$

Investigating $b_0 = 10$ with $b(s) = b_0(s + 1)$ by finding the root locus of equation 3.44 will show the following figure

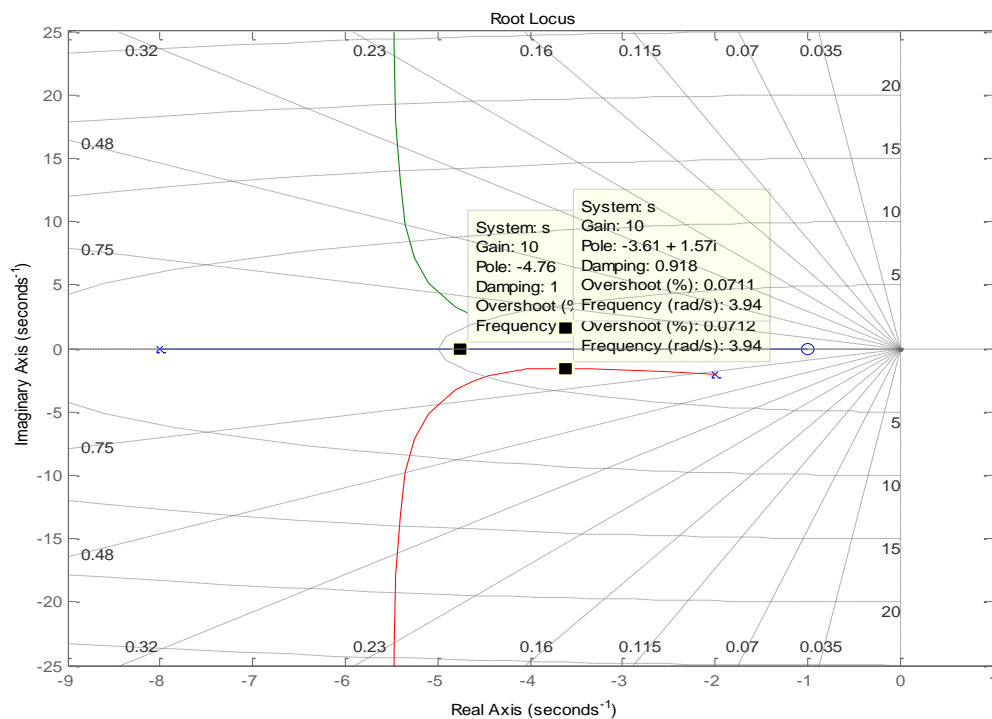


Figure 3.1: root locus expression of equation 3.44

The root locus in the previous page shows that the zero which is annotated as a circle pulls the pole towards it, as the gain is increased and the other poles in the imaginary part of the root locus will depart separately. The gain chosen in this design is $b_0 = 10$.

Finding the matrix Q requires the performance index become (J_{min}) in order to find the value n which minimizes $J(n)$. Then the numeric value for Q can be computed.

$$Q = \begin{bmatrix} 4 - 2n & 2 + n \\ 1 + 0.5n & n \end{bmatrix} \quad 3.45$$

The inverse matrix of Q is found to be

$$Q^{-1} = \begin{bmatrix} n & -2 - n \\ -1 - 0.5n & 4 - 2n \end{bmatrix} \frac{1}{4n - 2n^2 - (2 + n)(1 + 0.5n)} \quad 3.46$$

$$Q^{-1} = \frac{\begin{bmatrix} n & -2 - n \\ -1 - 0.5n & 4 - 2n \end{bmatrix}}{-2 + 2n - 2.5n^2} \quad 3.47$$

Then after obtaining Q and Q^{-1}

The equation below will be shown in the next page

$$J = \frac{(1 + n^2)(1 \quad 1) \begin{bmatrix} 1 + n + 1.25n^2 & -4 - 2n \\ -4 - 2n & 20 - 12n + 5n^2 \end{bmatrix} \begin{bmatrix} 1 \\ 1 \end{bmatrix}}{(-2 + 2n - 2.5n^2)^2}$$

Hence:

$$J = \frac{13 - 15n + 19n^2 - 15n^3 + 6.25n^4}{(-2 + 2n - 2.5n^2)^2} \quad 3.48$$

By using quotient rule the derivative of this equation is obtained

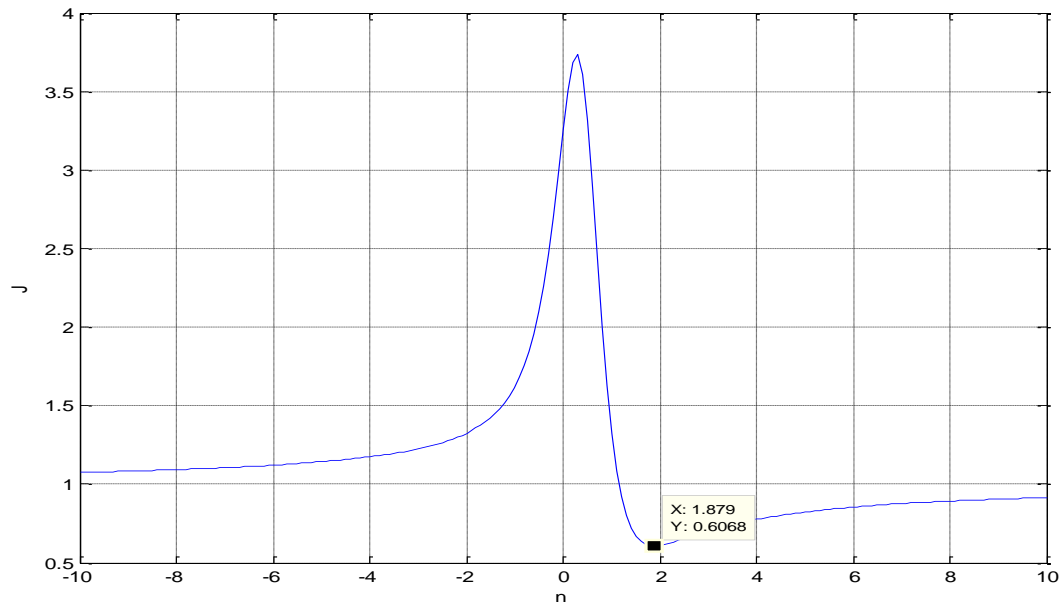


Figure 3.2: The Performance Index J against n

$$\frac{\partial J}{\partial n} = \frac{44 - 212n + 268n^2 - 285n^3 + 111.25n^4 - 62.5n^5 + 31.25n^6}{(-2 + 2n - 2.5n^2)^3} \quad 3.49$$

The minimum value as shown in figure 3.2 is chosen for the design of the low cost and low energy controller as mentioned in chapter two.

Now our $k_1 = 1, k_2 = n = 1.8795$ which represent the feed forward path

$$k = \begin{bmatrix} 1 \\ 1.8795 \end{bmatrix}, \quad h = Q^{-1} \begin{bmatrix} 1 \\ 1 \end{bmatrix} 10 = \begin{bmatrix} 2.829 \\ 2.404 \end{bmatrix},$$

$$P = [G(0)^{-1} + k \gg h] S_s [I - F S_s]^{-1}, \quad 3.50$$

and

$G(0) = \begin{bmatrix} 0.125 & -0.0625 \\ 0.03125 & 0.015625 \end{bmatrix}$. Additionally, when obtaining the inverse of the matrix, it will be shown as

$$G(0)^{-1} = \begin{bmatrix} 4 & 16 \\ -8 & 32 \end{bmatrix} \quad 3.51$$

The equation of Matrix S_s below should be positive so that the air flow is positive. Therefore, the value of S_s will be shown in the next page.

$$S_s = \begin{bmatrix} 1 & 0.1 \\ 0.1 & 1 \end{bmatrix} \quad 3.52$$

Applying the values of F on equations 3.9 and 3.50 will give

$$F = 0.1$$

$$P = \begin{bmatrix} 9.8695 & 21.3173 \\ 1.5243 & 40.2947 \end{bmatrix}$$

$$H = \begin{bmatrix} 0.1018 & 0.0015 \\ 0.1319 & 0.2121 \end{bmatrix}$$

$$F = 0.3$$

$$P = \begin{bmatrix} 13.5984 & 27.8489 \\ 3.6102 & 51.9405 \end{bmatrix}$$

$$H = \begin{bmatrix} 0.2981 & -0.0016 \\ 0.1025 & 0.3871 \end{bmatrix}$$

$$F = 0.5$$

$$P = \begin{bmatrix} 21.3644 & 40.3108 \\ 9.2807 & 73.4281 \end{bmatrix}$$

$$H = \begin{bmatrix} 0.4945 & -0.0047 \\ 0.0731 & 0.5621 \end{bmatrix}$$

The Optimum block diagram below will use the computation of the pre-compensator P Matrix, the values of k_1 and k_2 and also the values of h_1 and h_2 along with the value of F matrix. This model requires a simple time delay $= \frac{1}{2s+1}$ following input 2 as shown in figure 3.3 to avoid the swelling in the result for input 2 to output 1

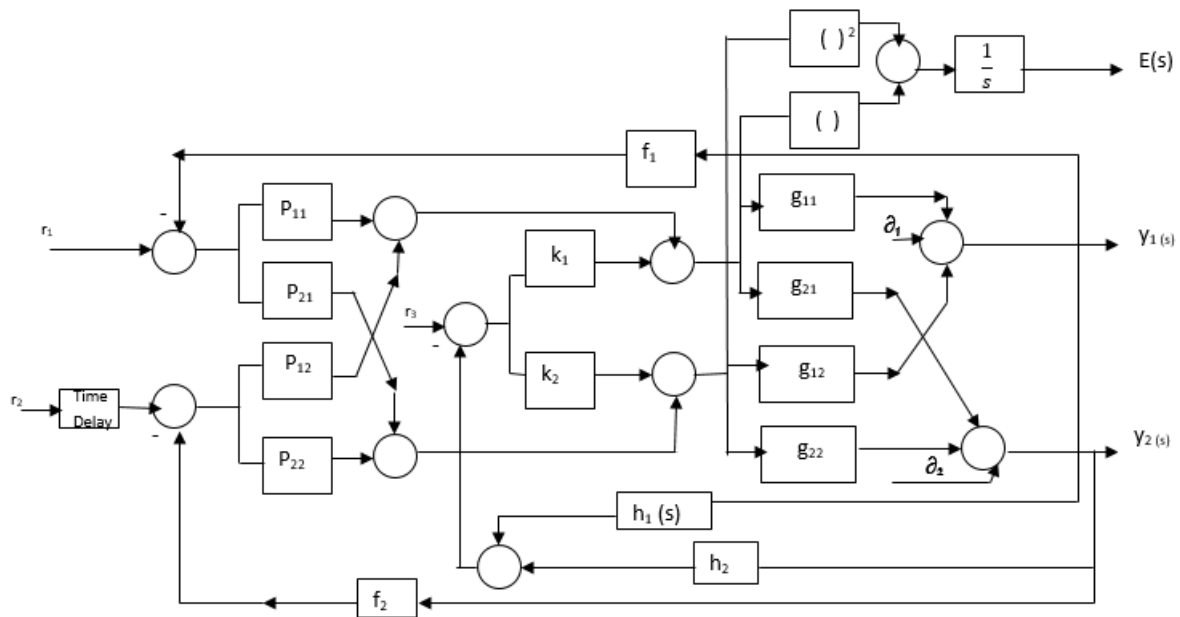


Figure 3.3: Block diagram representation of a Least Effort Controller for analysis purposes

Additionally, another block diagram which represents the conventional structure that uses the value of P which is represented by the value of K where $K=P$ is available. The conventional structure has a value of the feedback Matrix H that will be included in the following block diagram.

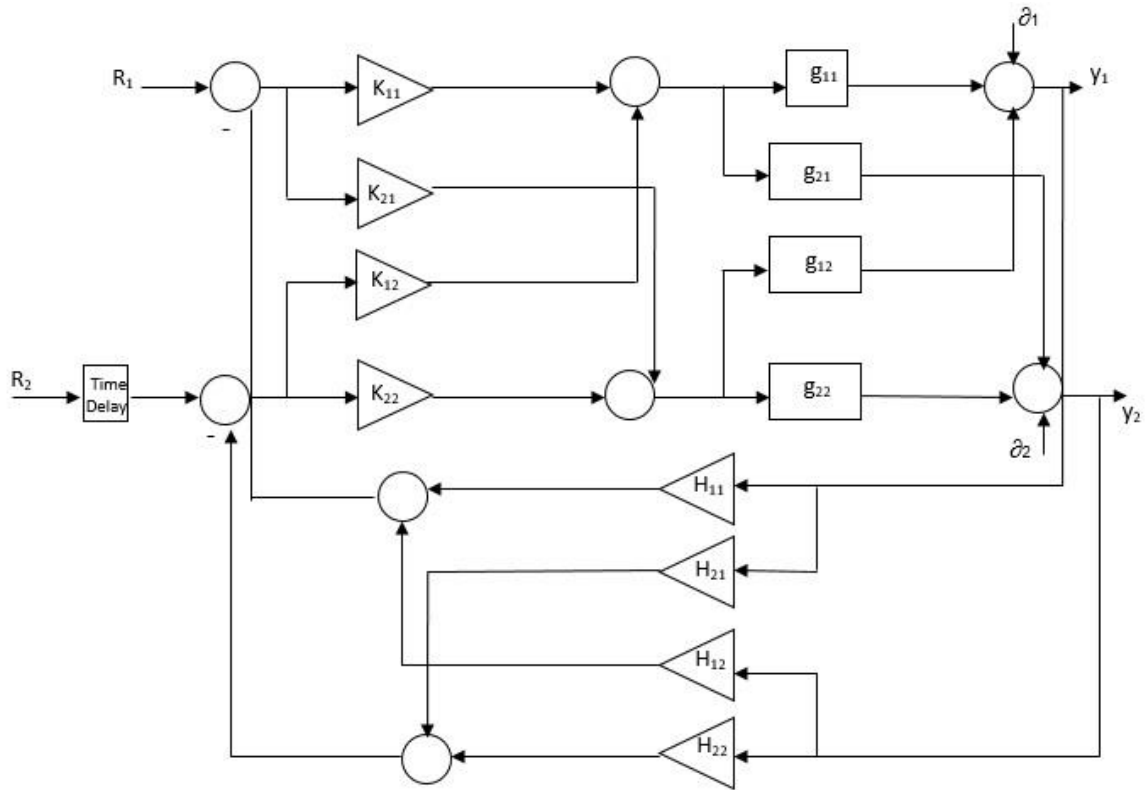


Figure 3.4: The Conventional Structure for a multivariable control system.

Chapter 4: Mathematical modelling using the Decoupling Compensator Control Method

4.1 Graph Details

In Order to determine the damping ratio and the natural frequency of the system, the oscillation must be found for the second input and second output frequency response where there is one oscillation without reference input time delay as shown in figure 4.1.

. The periodic time, damped natural frequency will be found and also the peak oscillation and damping ratio are will determined. Then, these equations will be applied in order to find the natural frequency. Finding the natural frequency will enable to find the forward path compensator of the system as will be shown in the following equations.

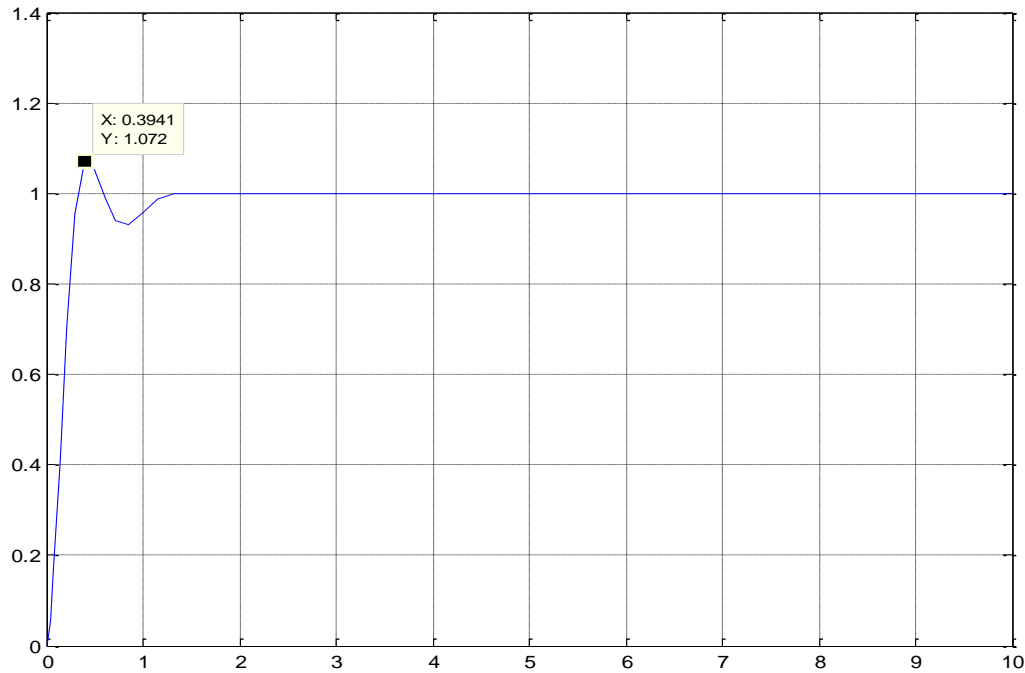


Figure 4.1: Time domain of input 2 and output 2 for $f=0.5$ in least effort controller without reference input time delay

From the figure in the previous page, the required parameters can be obtained in the equations that will be outlined below

$$T = 1.315 \text{ seconds}, \quad 4.1$$

$$\omega_d = 2\pi f = \frac{2\pi}{T} = 4.7781 \text{ rads/s}, \quad 4.2$$

$$h_1 = 0.072, \quad 4.3$$

and:

$$\zeta = \frac{1}{\sqrt{1 + \ln\left(\frac{h_1}{h_2}\right)}} \quad 4.4$$

But because there is only one overshoot the equations becomes

$$\zeta = \frac{1}{\sqrt{1 + \ln(h_1)}} = 0.3863 \quad 4.5$$

Applying the above equations in the equation below

$$\omega_n = \frac{\omega_d}{\sqrt{1 - \zeta^2}} \quad 4.6$$

So that

$$\omega_n = 5.1801 \text{ rads/s} \quad 4.7$$

4.2 Forward Path Compensator Analysis

Using the same system equation, the overall compensator can be determined for the other control method for the wind tunnel.

$$G(s) = \begin{bmatrix} \frac{1}{s^2 + 4s + 8} & \frac{0.5(s - 4)}{(s + 4)(s^2 + 4s + 8)} \\ \frac{2}{(s + 8)(s^2 + 4s + 8)} & \frac{s + 1}{(s + 8)(s^2 + 4s + 8)} \end{bmatrix} \quad 4.8$$

Inverting this matrix will give the pre-compensator matrix as follows

$$K_p(s) = G(s)^{-1} = \frac{1}{s^4 + 8s^3 + 32s^2 + 64s + 64} \begin{bmatrix} k_{11} & k_{12} \\ k_{21} & k_{22} \end{bmatrix} \quad 4.9$$

where

$$k_{11} = s^6 + 13s^5 + 76s^4 + 256s^3 + 512s^2 + 576s + 256$$

$$k_{21} = -2s^5 - 24s^4 - 128s^3 - 384s^2 - 640s - 512$$

$$k_{12} = -0.5s^6 - 6s^5 - 16s^4 + 32s^3 + 352s^2 + 896s + 1024$$

$$k_{22} = s^6 + 20s^5 + 160s^4 + 704s^3 + 1856s^2 + 2816s + 2048$$

For the forward path open-loop compensator the diagonal elements of it will be outlined as follows:

$$k_{d11}(s) = \frac{kn(s)}{kd(s)} \quad 4.10$$

So in close loop, the equation becomes

$$\frac{Y_1}{R_1}(s) = \frac{k_{d11}(s)}{1 + k_{d11}(s)} = \frac{kn(s)}{kd(s) + kn(s)} = \frac{\omega_n^2}{s^2 + 2\zeta\omega_n s + \omega_n^2} \quad 4.11$$

And the forward path compensator matrix will be shown as

$$K_d(s) = \begin{bmatrix} k_{d11} & 0 \\ 0 & k_{d22} \end{bmatrix} \quad 4.12$$

Applying equations 4.5 and 4.7 on equation 4.10 and 4.11 will give

$$\frac{Y_1}{R_1}(s) = \frac{26.8332}{s^2 + 4.002s + 26.8332} \quad 4.13$$

where $kn(s) = 26.8332$ and $kd(s) = s^2 + 4.002s$

$$\text{so that } K_d(s) = \begin{bmatrix} \frac{26.8332}{s^2+4.002s} & 0 \\ 0 & \frac{26.8332}{s^2+4.002s} \end{bmatrix} \quad 4.14$$

Then the overall compensator is

$$\begin{aligned} K_p K_d &= \frac{1}{s^4 + 8s^3 + 32s^2 + 64s + 64} \begin{bmatrix} k_{11} & k_{12} \\ k_{21} & k_{22} \end{bmatrix} \begin{bmatrix} k_{d11} & 0 \\ 0 & k_{d22} \end{bmatrix} = K_c \\ &= \frac{1}{s^6 + 12s^5 + 64.02s^4 + 192.1s^3 + 320.1s^2 + 256.1s} \begin{bmatrix} k_{c11} & k_{c12} \\ k_{c21} & k_{c22} \end{bmatrix} \quad 4.15 \end{aligned}$$

where

$$k_{c11} = 26.83s^6 + 348.8s^5 + 2039s^4 + 6869s^3 + 1.374 * 10^4 s^2 + 1.546 * 10^4 s + 6869$$

$$k_{c21} = -53.67 s^5 - 644 s^4 - 3435 s^3 - 1.03 * 10^4 s^2 - 1.717 * 10^4 s - 1.374 * 10^4$$

$$k_{c12} = -13.42 s^6 - 161 s^5 - 429.3 s^4 + 858.7 s^3 + 9445s^2 + 2.404 * 10^4 s + 2.748 * 10^4$$

$$\begin{aligned} k_{c22} &= 26.83 s^6 + 536.7 s^5 + 4293 s^4 + 1.889 * 10^4 s^3 + 4.98 * 10^4 s^2 + 7.556 * 10^4 s \\ &\quad + 5.495 * 10^4 \end{aligned}$$

The computation of the Decoupling compensator matrix terms will be applied in figure 4.1 next page and the response for both outputs corresponding to the step change in inputs 1 and 2.

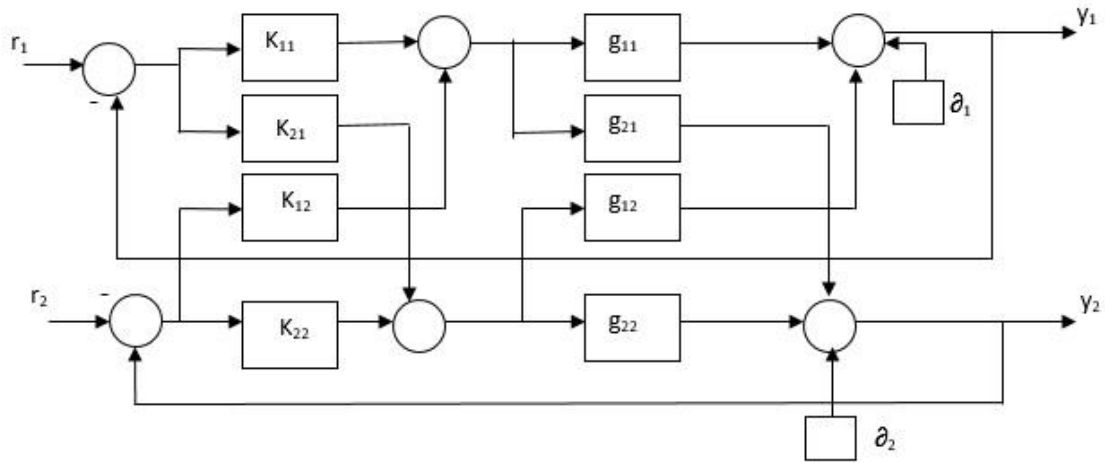


Figure 4.2: Decoupled control system Block Diagram

Chapter 5: Results and Discussion

5.1 Results and Discussion

In this chapter, the outcome of the design in the previous chapter will be shown below

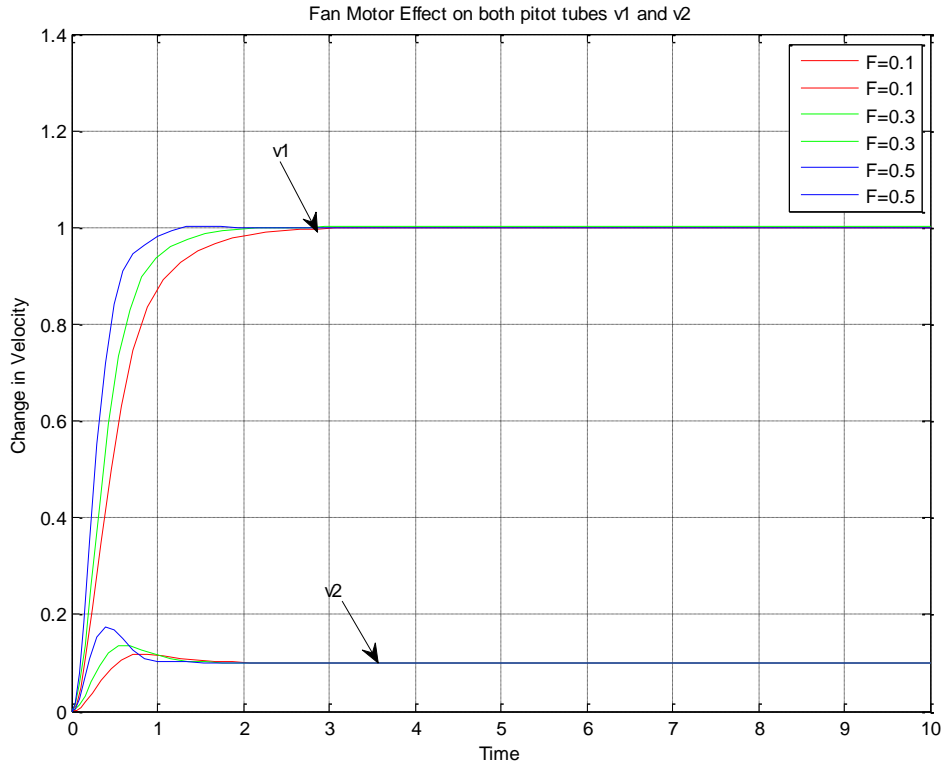


Figure 5.1: System response following a unit step change on reference input r_1

In the figure above, the comparison of the three outer-loop feedback was made; which indicates that the outer-loop feedback $f=0.1$ is the slowest in the transient response than the other two outer-loop feedbacks $f=0.3$ and $f=0.5$ while $f=0.5$ is the fastest among them in the pitot tube v_1 . There are no oscillations in the three of them so the steady state errors are eliminated from them and they are overdamped as well. In Pitot tube v_2 it is found that $f=0.5$ has a slight oscillation amongst the others which are even lower in oscillation $f=0.3$ down to $f=0.1$. It is also seen that $f=0.3$ goes to steady state faster than the others. This is also true when compared to the wind tunnel design.

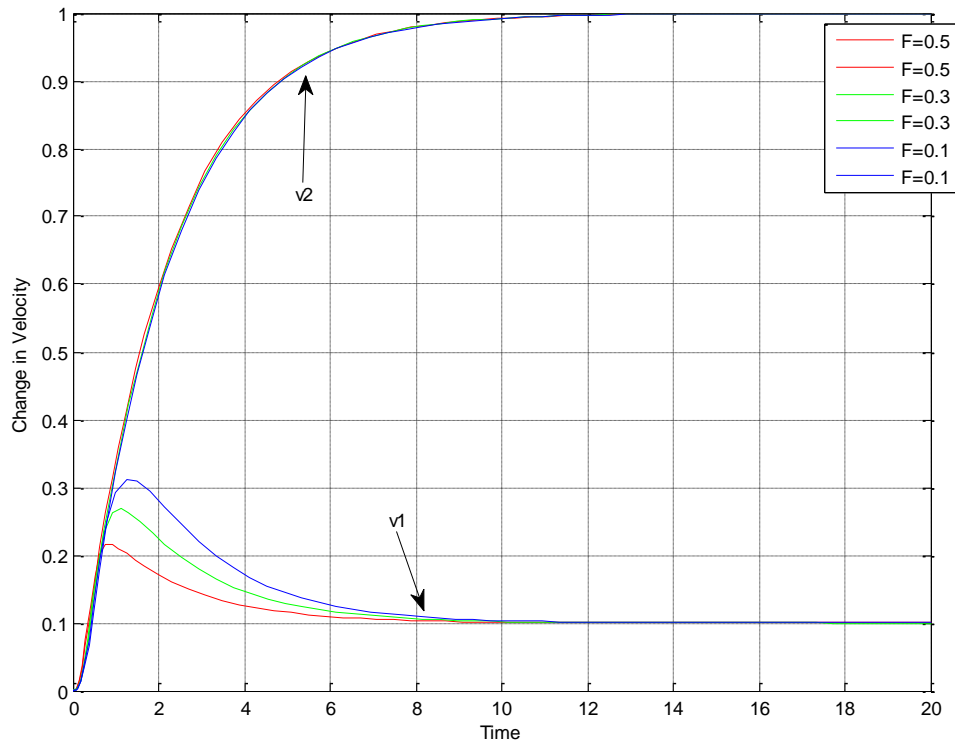


Figure 5.2: System response following a unit step change on reference input r_2 .

As seen in the figure above, the boost in v_1 was reduced and also the oscillation of v_2 was eliminated. For $f=0.1, 0.3$ and 0.5 in v_2 , it can be seen that all of them have the same rise-time and settling time. In v_1 it can be seen that $f=0.1$ has the highest oscillation and $f=0.5$ has the lowest oscillation. The time delay used has the transfer function of $(1/2s+1)$.

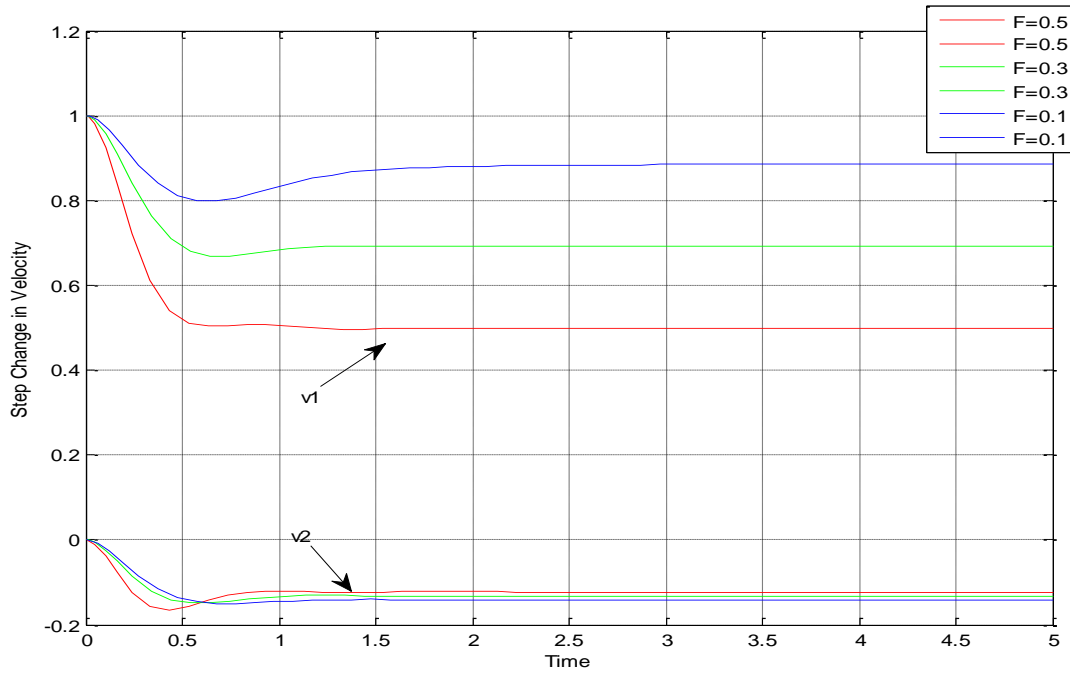


Figure 5.3: System response following a unit step change on δ_1

The figure above shows the disturbance suppression for the three outer-loop feedback gains on v_1 and v_2 of the fan motor. The plot in v_1 shows that $f=0.5$ is the best in recovery amongst the all three of them with no oscillations as well. It also goes to a steady state faster than the others. In v_2 only $f=0.1$ is a little bit better in recovery than $f=0.3$ and $f=0.5$ and a bit faster than both. But it is still recommended to choose the outer-loop feedbacks between $f=0.3$ and $f=0.5$ for both outputs.

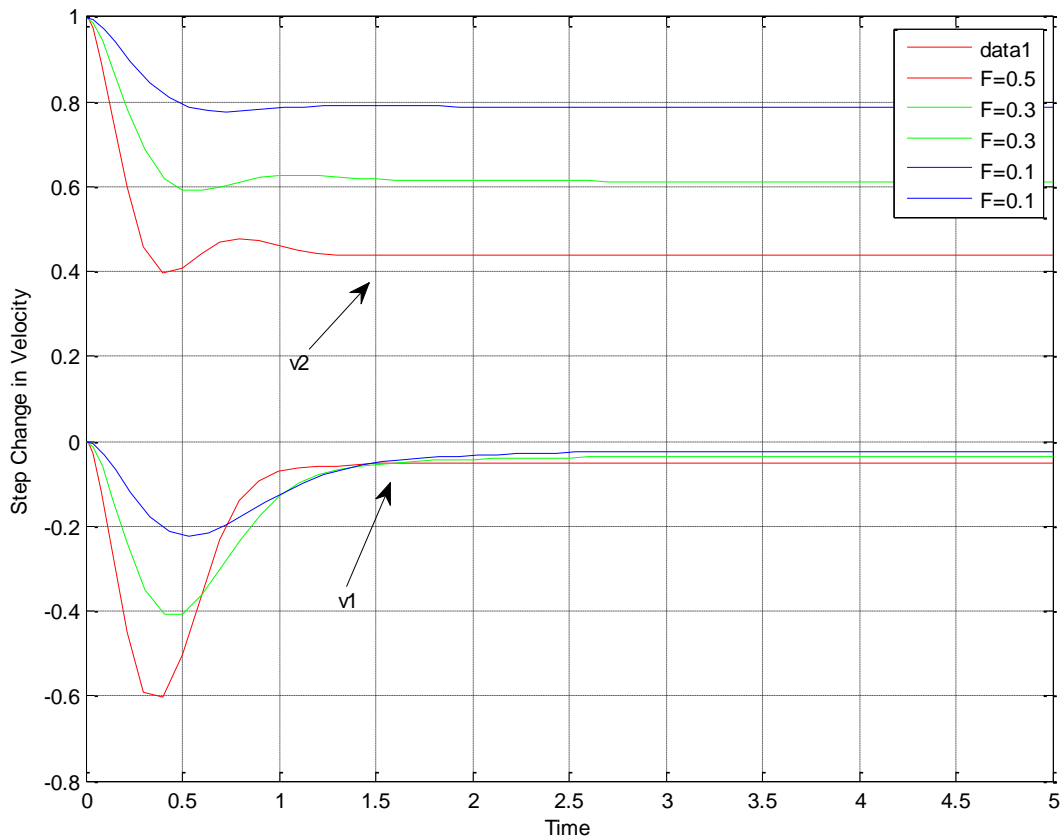


Figure 5.4: System response following a unit step change on δ_1

The effect of disturbance 2 on v_2 plot shows that there is some oscillation on $f=0.5$ and less in $f=0.3$ until there is no oscillation on $f=0.1$. However, the recovery of the outer-loop feedback gains $f=0.5$ and $f=0.1$ are faster than $f=0.3$. For v_1 more $f=0.5$ has the biggest oscillation amongst the other feedback gains but it recovers faster than them. Feedback gain $f=0.3$ has less oscillation than $f=0.5$ and faster than $f=0.1$ in recovery, whereas $f=0.1$ has least oscillation but slowest in disturbance recovery.

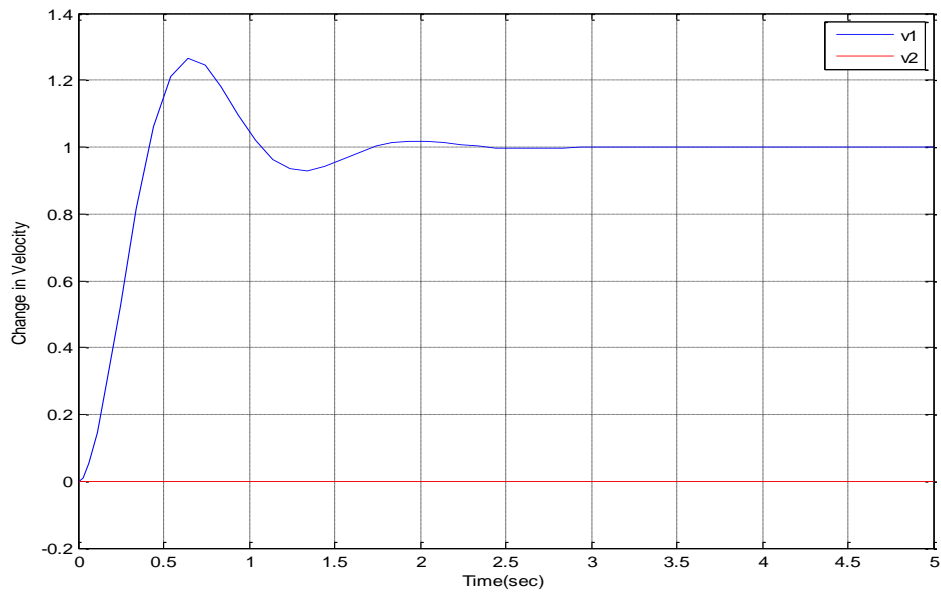


Figure 5.5: System response following a unit step change on reference input r_1 for the decoupling compensator

It is shown in figure 5.5 that input 1 will have a direct effect on v_1 while the effect on v_2 is completely neutralized. This means the decoupling of v_2 has been successfully achieved.

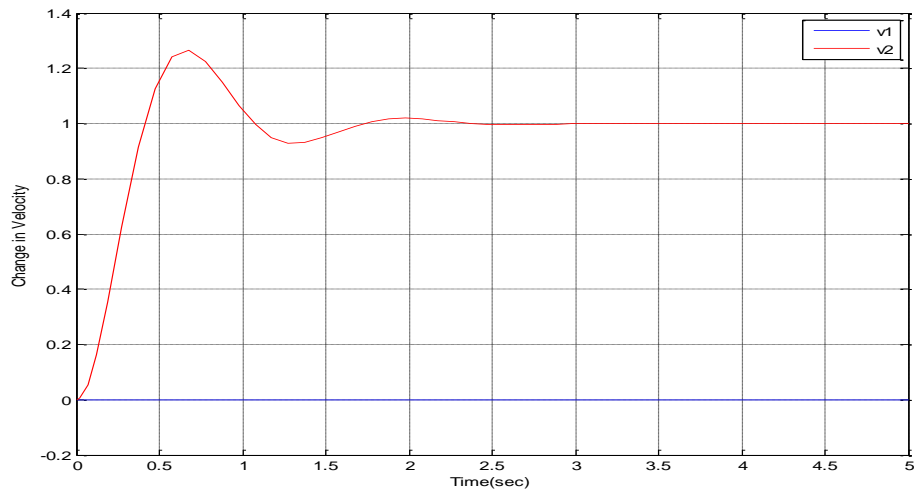


Figure 5.6: System response following a unit step change on reference input r_1 for the decoupling compensator

It is shown in figure 5.6 that input 2 will have a direct effect on v_2 while the effect on v_1 is completely neutralized. This means the decoupling of v_1 has been successfully achieved.

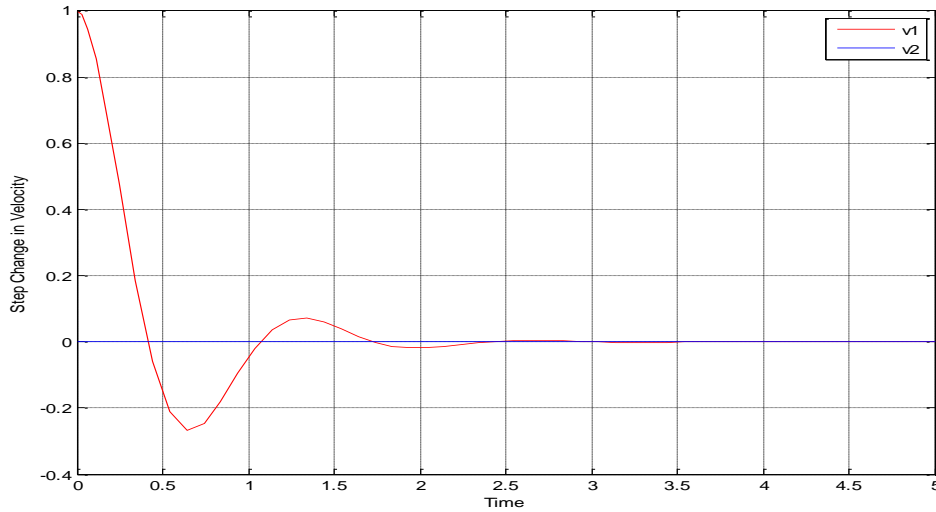


Figure 5.7: System response following a unit step change on ∂_1 for the decoupling compensator

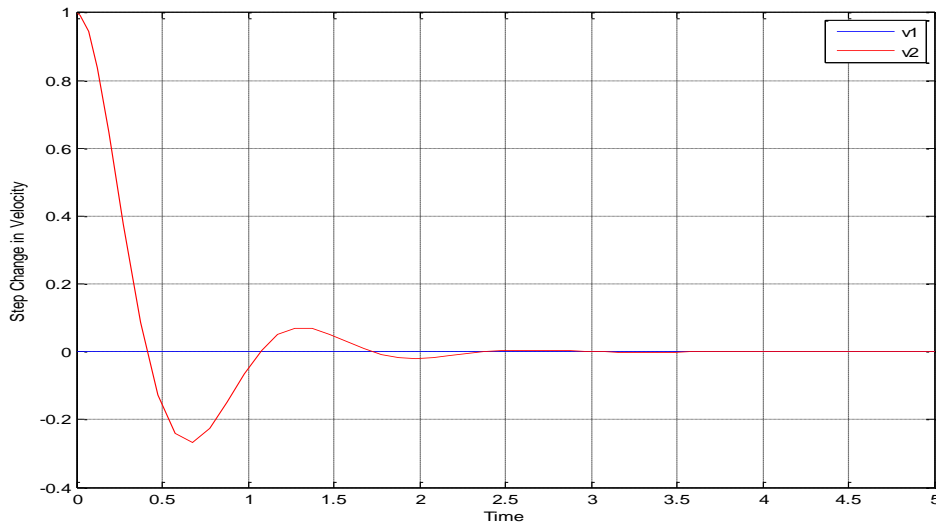


Figure 5.8: System response following a unit step change on ∂_2 for the Decoupling compensator

In both figures 5.6 and 5.7, it can be seen that the disturbance has no effect on v_2 and v_1 respectively and that is because both are completely decoupled. It can be seen that the disturbance is completely rejected for both v_1 and v_2 respectively. However, the settling time and the oscillation are very high.

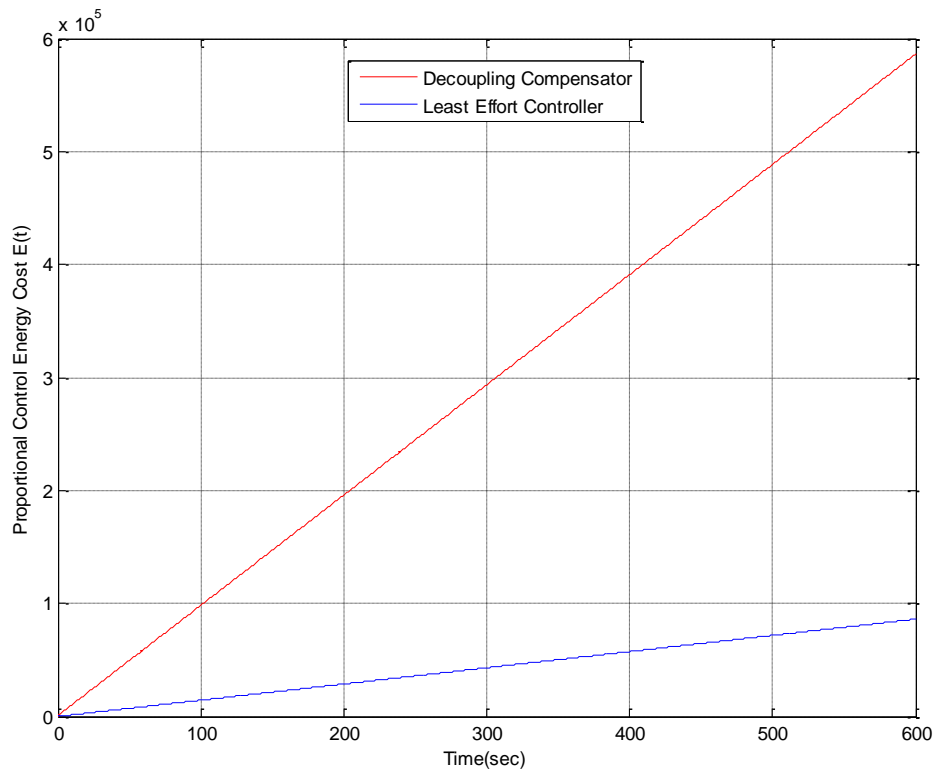


Figure 5.9: Proportional control energy costs following random distribution on disturbances 1 and 2 for the Least Effort Controller and the Decoupling Compensator.

5.2 Summary

Overall, it is concluded that every method of control has its conditions and different ways to design a certain controller. Additionally, each method has its unique modelling and ways to determine a suitable controller. These equations and findings were illustrated as graphs representing responses of each method, disturbance rejection for each method and comparisons were made.

It is also concluded that the Decoupling compensator method has a very high order which means it is not practical whereas the least effort controller pre compensator is only numeric and hence it can be used in practice as the results show. The decoupling controller also gives oscillatory response. Additionally, both figures 5.7 and 5.8 show that the disturbance recovery is very slow; whereas the figures 5.3 and 5.4 show that the disturbance recovery is much faster in all conditions for the least effort controller.

As in the figure 5.9 it shows that the energy cost in the least effort controller is dramatically less than the decoupling compensator. Therefore it is again proven that the least effort controller has least maintenance cost than the decoupling compensator and the other methods that were shown in figure 2.8 in chapter 2.

Chapter 6: Conclusion & Recommendation

6.1 Conclusion

Once again as can be seen from the plots of chapter 5 that illustrate the least effort control method has fulfilled the requirement of the project as it is very stable, reliable and cost effective. The response is fast and stable without the need to add any other components to the system to get rid of oscillations. Moreover, the overshoot percentage is below 10% percent, which is required for practicality. This method makes it easier to control the fan motor and ventilation vane angles without worrying about the energy dissipated. This also means less times and costs of maintenance.

The least effort control method proves compared to the compensator method that it dissipates less control energy. The Decoupling compensator dissipates a very large amount of energy compared to the least effort controller as shown in figure 5.9 and is more difficult to control the air velocity with it than with the proposed controller. The outer-loop of the design was configured for a steady state output aiming for an overdamped behavior and good disturbance recovery with feedback gains set to $f_1=f_2=0.5$, while the Decoupling compensator method is not suitable for disturbance rejection as seen in figures 5.6 and 5.7.

6.2 Recommendation

The proposed least effort controller is recommended for the future applications on wind tunnels as this should be a safest, most cost effective and reliable method as severe turbulences sometimes occur in any air transportation, Accurate measurement of the aircraft design in order to prevent any danger especially in long journeys. The control of the air flow in the wind tunnel should be stable for the ease of the design of certain aircraft components. Accurate air flow control means easier aircraft behavior measurements, for air flow velocity changes. Least effort control overall is recommended for more complex systems with more than two inputs and outputs. The Decoupling compensator requires a very high polynomial controller order to design the forward path compensator. Therefore, it is not recommended for use at all as it is very huge, impractical and uses lots of energy which will continuously require maintenance unlike the least effort controller that is designed by only using scaler for the pre-compensator.

REFERENCES

1. Albertos, P. and Sala, A. (2004). *Multivariable control systems*. London: Springer.
2. Anderson, J. (2001). *A history of aerodynamics and its impact on flying machines*. Cambridge [u.a.]: Cambridge Univ. Press.
3. Bennett, S. (1993). *A history of control engineering, 1930-1955*. Stevenage, Herts., U.K.: P. Peregrinus on behalf of the Institution of Electrical Engineers, London.
4. Burghes, D. and Graham, A. (n.d.). *Control and optimal control theories with applications*.
5. Ghosh, S. (2007). *Control Systems: Theory and Applications*. Punjab: Pearson Education.
6. Gopal, M. (1993). *Modern control system theory*. New York: Wiley.
7. Green, J. and Quest, J. (2011). A short history of the European Transonic Wind Tunnel ETW. *Progress in Aerospace Sciences*, 47(5), pp.319-368.
8. Harsch, V., Bardrum, B. and Illig, P. (2008). Lilienthal's Fatal Glider Crash in 1896: Evidence Regarding the Cause of Death. *aviat space environ med*, 79(10), pp.993-994.
9. *How WIND TUNNELS Work - F1 explained- Sauber F1 Team*. (2014). [video] Sauber F1 Team. URL: <https://www.youtube.com/watch?v=KC0E0wU6inU>.
10. Dutton, K, Thompson, S, Barraclough, W (June 6, 1997). *The Art of Control Engineering*. Edinburgh: Prentice Hall; 1 edition (June 6, 1997).
11. Miguel, A. González, H. Ana I. López, M. Jarzabek, A. José, M. Sun, X, and Yuliang, W. (2013). *Design Methodology for a Quick and Low-Cost Wind Tunnel*. INTECH Open Access Publisher.
12. Paraschivoiu, I. (2003). "*Subsonic aerodynamics*". Montreal: Presses internationales Polytechnique.
13. Whalley, R. and Ebrahimi, M. (2006). "*Multivariable System Regulation*", Proc.IMEch E pt C, Vol 120, 2006, pp.653-667.

14. Whalley, R. and Mitchell, D. (1996). “*The identification of engineering system parameters*”, Proc.IMEch E pt C, Vol 211, pp.1-13.
15. Hussain, D. and Hamid A. (2014). Testing and Commissioning of a Low-Speed Wind Tunnel (LSWT) Test Section. *Journal of Engineering*, [online] 20(11). Available at: <http://www.iasj.net/iasj?func=fulltext&aId=94409> [Accessed 14 Aug. 2015].

